Next-to-modified leading logarithmic approximation corrections to single inclusive $k_\perp$ distributions and two-particle correlations in a jet

Redamy Pérez-Ramos,[1,2,‡] François Arleo,[3,§] and Bruno Machet[4,‖]

[1]*Max-Planck-Institut für Physik, Werner-Heisenberg-Institut, Föhringer Ring 6, D-80805 München, Germany*
[2]*Present address: II.Institut für Theoretische Physik, Universität Hamburg, Lupurer Chaussee 149, D-22761 Hamburg, Germany*
[3]*LAPTH[*], Université de Savoie et CNRS, 9 chemin de Bellevue, BP110, 74941 Annecy-le-Vieux Cedex, France*
[4]*Laboratoire de Physique Théorique et Hautes Énergies[+], UPMC Univ Paris 06, BP 126, 4 place Jussieu F-75252 Paris Cedex 05, France*

(Received 15 January 2008; published 25 July 2008)

The hadronic $k_\perp$-spectrum inside a high-energy jet is determined including corrections of relative magnitude $\mathcal{O}(\sqrt{\alpha_s})$ with respect to the Modified Leading Logarithmic Approximation (MLLA) in the limiting spectrum approximation (assuming an infrared cutoff $Q_0 = \Lambda_{\rm QCD}$) and beyond ($Q_0 \neq \Lambda_{\rm QCD}$). The results in the limiting spectrum approximation are found to be, after normalization, in impressive agreement with preliminary measurements by the CDF Collaboration, unlike what occurs at MLLA, pointing out small overall nonperturbative contributions. Within the same framework, 2-particle correlations inside a jet are also predicted at next-to-MLLA and compared to previous MLLA calculations.

DOI: 10.1103/PhysRevD.78.014019 PACS numbers: 12.38.Cy, 13.87.−a, 13.87.Fh

I. INTRODUCTION

The production of jets—a collimated bunch of hadrons—in e^+e^-, e^-p and hadronic collisions is an ideal playground to investigate the parton evolution process in perturbative QCD (pQCD). One of the great successes of pQCD is the existence of the hump-backed shape of inclusive spectra, predicted in [1] within the Modified Leading Logarithmic Approximation (MLLA), and later discovered experimentally (for review, see e.g. [2]). Refining the comparison of pQCD calculations with jet data taken at LEP, Tevatron and LHC will ultimately allow for a crucial test of the Local Parton Hadron Duality (LPHD) hypothesis [3] and for a better understanding of color neutralization processes.

Progress towards this goal has been achieved recently. On the theory side, the inclusive $k_\perp$-distribution of particles inside a jet has been computed at MLLA accuracy [4], as well as correlations between two particles in a jet [5]. Analytic calculations have first been done in the limiting spectrum approximation, i.e. assuming an infrared cutoff Q_0 equal to $\Lambda_{\rm QCD}$ ($\lambda \equiv \ln Q_0/\Lambda_{\rm QCD} = 0$). Subsequently, analytic approximations for correlations were obtained beyond the limiting spectrum using the steepest descent method [6]. Experimentally, the CDF Collaboration at Tevatron reported on $k_\perp$-distributions of unidentified hadrons in jets produced in $p\bar{p}$ collisions at $\sqrt{s} = 1.96$ TeV [7].

MLLA corrections, of relative magnitude $\mathcal{O}(\sqrt{\alpha_s})$ with respect to the leading double logarithmic approximation (DLA), were shown to be quite substantial for single-inclusive distributions and 2-particle correlations [4,5]. Therefore, it appears legitimate to wonder whether corrections of order $\mathcal{O}(\alpha_s)$, that is next-to-next-to-leading or next-to-MLLA (NMLLA), are negligible or not.

The starting point of this analysis is the MLLA evolution equation for the generating functional of QCD jets [8]. Together with the initial condition at threshold, it determines jet properties at all energies. At high energies one can represent the solution as an expansion in $\sqrt{\alpha_s}$. Then, the leading (DLA) and next-to-leading (MLLA) approximations are complete. The next terms (NMLLA) are not complete but they include an important contribution which takes into account energy conservation and an improved behavior near threshold. An example of a solution for the single-inclusive spectrum from the MLLA equation is the so-called "limiting spectrum" (for a review, see [8]) which represents a perturbative computation of the spectrum at $\lambda = 0$ with complete leading and next-to-leading asymptotics. Some results for such NMLLA terms have been studied previously for global observables and have been found to better account for recoil effects. They were shown to drastically affect multiplicities and particle correlations in jets: this is, in particular, the case in [9], which deals with multiplicity correlators of order 2, and in [10], where multiplicity correlators involving a higher number of partons are studied; in particular, the higher this number, the larger turn out to be NMLLA corrections.

The present study makes use of this evolution equation to estimate NMLLA contributions to our differential observables. It presents the complete calculations of the single-inclusive $k_\perp$-distribution leading to the main results

[*]Laboratoire de Physique Théorique d'Annecy-le-Vieux, UMR 5108
[+]LPTHE, UMR 7589 du CNRS associée à l'Université P. et M. Curie - Paris 6
[‡]redamy@mail.desy.de
[§]arleo@lapp.in2p3.fr
[‖]machet@lpthe.jussieu.fr

published in [11], and extends them to 2-particle correlations inside a high-energy jet.

The paper is organized as follows. First, Sec. II presents a system of evolution equations including $\mathcal{O}(\alpha_s)$ corrections, which allows for the computation of the inclusive spectrum, G, beyond MLLA accuracy. Section III is devoted to the NMLLA evaluation of the color currents of quark and gluon jets and, from them, to the inclusive $k_\perp$-distribution in the limiting spectrum approximation. These predictions are also compared to preliminary measurements performed recently by the CDF Collaboration. Going beyond the limiting spectrum is the subject of Sec. IV, in which inclusive $k_\perp$-distributions are computed at an arbitrary λ. The 2-particle correlations including NMLLA corrections are determined in Sec. V. Finally, the present approach and the results obtained in this paper are discussed in detail and summarized in Sec. VI.

II. EVOLUTION EQUATIONS

A. Logic and energy conservation

As a consequence of the probabilistic shower picture, the notion of *Generating Functional* (GF) was proved suitable to understand and includes higher-order corrections to DLA asymptotics (see [8] and references therein).

The single-inclusive spectrum and the n-particle momentum correlations can be derived from the MLLA Master Equation for the GF $Z = Z(u)$ [8] after successively differentiating with respect to a certain *probing* function $u = u(k)$; k denotes the quadri-momentum of one parton inside the shower and the solutions of the equations are written as a perturbative expansion in α_s. At high energies this expansion can be resummed and the leading contribution can be represented as an exponential of the anomalous dimension $\gamma(\alpha_s)$; since further details to this logic can be found in [5,8], we only give the symbolic structure of the equation for the GF and its solution as

$$\frac{dZ}{dy} \simeq \gamma_0(y)Z \Rightarrow Z \simeq \exp\left\{\int^y \gamma(\alpha_s(y'))dy'\right\} \qquad (1)$$

where $\gamma(\alpha_s)$ can be written as an expansion in powers of $\sqrt{\alpha_s}$

$$\gamma(\alpha_s) = \sqrt{\alpha_s} + \alpha_s + \alpha_s^{3/2} + \alpha_s^2 + \ldots. \qquad (2)$$

The equation in (1) applies to each vertex of the cascade and its solution represents the fact that successive and independent partonic splittings inside the shower, such as the one displayed in Fig. 1, exponentiate with respect to the *evolution-time* parameter $dy = d\Theta/\Theta$; $\Theta \ll 1$ is the angle between outgoing couples of partons. The choice of y follows from Angular Ordering (AO) in intrajet cascades; it is indeed the suited variable for describing *timelike* evolution in jets. Thus, Eq. (1) incorporates the Markov chains of sequential angular ordered partonic decays which

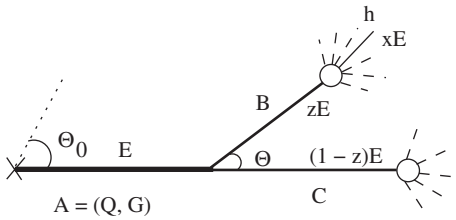

FIG. 1. Parton A with energy E splits into parton B (respectively, C) with energy zE (respectively, $(1-z)E$) which fragments into a hadron h with energy xE.

are singular in Θ and $\gamma(\alpha_s)$ determines the rate of inclusive quantities growth with energy.

While DLA treats the emission of both particles as independent by keeping track of the first term $\sim\sqrt{\alpha s}$ in (2) without constraint, the exact solution of the MLLA evolution equation (partially) fulfills the energy conservation in each individual splitting process $(z + (1-z) = 1)$ by incorporating higher-order $(\alpha_s^{n/2},\ n > 1)$ terms to the anomalous dimension. Symbolically, the first two analytical steps towards a better account of these corrections in the MLLA, NMLLA evolution, which we further discuss in Sec. II C, can be represented in the form

$$\Delta\gamma \simeq \int(\alpha_s + \alpha_s\ell^{-1}\ln z)dz \sim \alpha_s + \alpha_s^{3/2},$$

where $\ell = \ln(1/x) \sim \alpha_s^{-1/2}$ with $x \ll 1$ (fraction of the jet energy taken away by one hadron), $z \sim 1$ for hard parton splittings such as $g \to q\bar{q}\ldots$ (this is in fact the region where the two partons are strongly correlated).

Energy conservation is particularly important for energetic particles as the remaining phase space is then very limited. On the other hand, a soft particle can be emitted with little impact on energy conservation. Some consequences of this behavior have also been noted in [12]:

(i) the soft particles follow the features expected from DLA;
(ii) there is no energy dependence of the soft spectrum;
(iii) the ratio of soft particles $r = N_g/N_q$ in gluon and quark jets is consistent with the DLA prediction $N_c/C_F = 9/4$ (see the measurement by DELPHI [13]).

This is quite different from the ratio of global multiplicities which acquires large corrections beyond DLA (see, for example, Fig. 18 in the second reference given in [14]). For this quantity the HERWIG parton shower model corresponding to MLLA and exact energy conservation (same Fig. 18) and the full summation of the perturbative series of MLLA evolution equation (see also [15]) come close to the data at $r = N_g/N_q \approx 1.5$ at LEP energies. As an intermediate example, we can mention the successful description of the semisoft particle $\ln(1/x)$ distribution (''hump-backed plateau'') where the first correction (MLLA), despite the large value of the expansion

parameter $\sqrt{\alpha_s} \approx 0.35$, already gives a good description of the data at the Z^0 peak ($Q = 91.2$ GeV) of the e^+e^- annihilation into a $q\bar{q}$ pair [16].

B. MLLA evolution

We study the formation of hadrons inside a jet produced in high-energy scattering processes, such as e^+e^- annihilation or pp and $p\bar{p}$ collisions. A jet of total opening angle Θ_0 is initiated by a parton A (either a quark, Q, or a gluon, G) with energy E; A then splits into partons B and C, with energy fractions z and $(1-z)$, respectively, forming a relative angle Θ (see Fig. 1). At the end of the cascading process, the parton B fragments into a hadron h with energy xE, with the fragmentation function

$$B(z) = \frac{x}{z} D_{\mathrm{B}}^{h}\left(\frac{x}{z}, zE\Theta_0, Q_0\right), \qquad (B = Q, G) \tag{3}$$

which describes the distribution of the hadron h inside the subjet B with an energy-fraction x/z.

As a consequence of AO in parton cascades, the functions $Q(z)$ and $G(z)$ satisfy the system of two-coupled integro-differential evolution equations [5]:

$$Q_y \equiv \frac{dQ}{dy} = \int_0^1 \mathrm{d}z \frac{\alpha_s}{\pi} \Phi_q^g(z)[(Q(1-z) - Q) + G(z)], \tag{4}$$

$$\begin{aligned} G_y &\equiv \frac{dG}{dy} \\ &= \int_0^1 \mathrm{d}z \frac{\alpha_s}{\pi} [\Phi_g^g(z)(1-z)(G(z) + G(1-z) - G) \\ &\quad + n_f \Phi_g^q(z)(2Q(z) - G)], \end{aligned} \tag{5}$$

with α_s, the running coupling constant of QCD, given by

$$\alpha_s \equiv \alpha_s(\ell, y) = \frac{2\pi}{4N_c\beta_0(\ell + y + \lambda)}, \tag{6}$$

and where we define

$$\ell = \ln(1/x), \qquad y = \ln\frac{k_\perp}{Q_0} = \ln\frac{xE\Theta_0}{Q_0}, \qquad \lambda = \ln\frac{Q_0}{\Lambda_{\mathrm{QCD}}}, \tag{7}$$

following the notations of Ref. [8]; the MLLA equations above follow from the GF logic commented upon in the introductory paragraph. The scale Q_0 appearing in (7) is the collinear cutoff parameter, Λ_{QCD} is the nonperturbative scale of QCD which we set to 250 MeV in this work [17], and

$$\beta_0 = \frac{1}{4N_c}\left(\frac{11}{3}N_c - \frac{4}{3}T_R\right) \tag{8}$$

is the first term in the perturbative expansion of the β-function (N_c is the number of colors, $T_R = n_f/2$ where $n_f = 3$ is the number of light quark flavors). We only consider in this work the 1-loop expression for the running coupling constant, assuming that the role of the conservation of energy is much more important than the effects of 2-loop corrections to α_s, as seen for instance in the case of multiplicity distributions [14]; we shall discuss this further in Sec. VI A. The coupling constant α_s is also linked to the DLA anomalous dimension γ_0 of twist-2 operators by

$$\begin{aligned} \gamma_0^2(\ell, y) &= 2N_c \frac{\alpha_s(\ell, y)}{\pi} = \frac{1}{\beta_0(Y_\Theta + \lambda)}, \\ Y_\Theta &= \ell + y = \ln\frac{E\Theta}{Q_0}. \end{aligned} \tag{9}$$

In Eqs. (4) and (5), $\Phi_{\mathrm{A}}^{\mathrm{B}}(z)$ represent the 1-loop DGLAP splitting functions [8] and we note:

$$\begin{aligned} Q \equiv Q(1) &= xD_q^h(x, E\Theta_0, Q_0), \\ G \equiv G(1) &= xD_g^h(x, E\Theta_0, Q_0). \end{aligned}$$

In the small $x \ll z$ limit which we consider here, the fragmentation functions behave as

$$B(z) \overset{x\ll z}{\approx} \rho_{\mathrm{B}}^h\left(\ln\frac{z}{x}, \ln\frac{zE\Theta_0}{Q_0}\right) = \rho_{\mathrm{B}}^h(\ln z + \ell, y), \tag{10}$$

where ρ_{B}^h is a slowly varying function of the two logarithmic variables $\ln(z/x)$ and y [1] that describes the humpbacked plateau.

C. Taylor expansion

The resummation scheme at MLLA is discussed in [5], in which $G(z)$ and $G(1-z)$ were replaced by $G(1)$ in the nonsingular part of the integrands in Eqs. (4) and (5). In the present work, we calculate next-to-MLLA corrections from the Taylor expansion of ρ_{B}^h in the variables $\ln z$ and $\ln(1-z)$ in the domain:

$$z \sim 1 - z \sim 1, \qquad x \ll 1 \Rightarrow \ell \gg |\ln z| \sim |\ln(1-z)|$$

corresponding to hard parton splittings. To first order,

$$\rho(\ln z) = \rho(\ln z = 0) + \left.\frac{\partial\rho(\ln z)}{\partial \ln z}\right|_{\ln z = 0} \ln z + \mathcal{O}(\ln^2 z), \tag{11}$$

$$\begin{aligned} \rho(\ln(1-z)) &= \rho(\ln(1-z) = 0) \\ &\quad + \left.\frac{\partial\rho(\ln(1-z))}{\partial \ln(1-z)}\right|_{\ln(1-z)=0} \ln(1-z) \\ &\quad + \mathcal{O}(\ln^2(1-z)), \end{aligned} \tag{12}$$

or, equivalently, for the function $B(z)$:

$$B(z) \overset{|\ln z| \ll \ell}{\approx} B(1) + B_\ell(1) \ln z + \mathcal{O}(\ln^2 z), \tag{13}$$

$$\begin{aligned} B(1-z) &\overset{|\ln(1-z)| \ll \ell}{\approx} B(1) + B_\ell(1) \ln(1-z) \\ &\quad + \mathcal{O}(\ln^2(1-z)). \end{aligned} \tag{14}$$

The derivative with respect to $\ln z$ or $\ln(1-z)$ has been replaced by the one with respect to ℓ because of (10) and the property that, at low x, B is a function of $(\ln z + \ell)$ or $(\ln(1-z)+\ell)$. Since $\ell = \mathcal{O}(1/\sqrt{\alpha_s})$ (see [8]) the above expansion can be written symbolically,

$$B(z) \sim B(1-z) \simeq c_1 + c_2(\sqrt{\alpha_s}) + \mathcal{O}(\alpha_s),$$
$$c_1, c_2 = \mathcal{O}(1).$$

The terms proportional to B_ℓ thus provide NMLLA corrections to the solutions of the MLLA evolution Eqs. (4) and (5).

D. Evolution equations including NMLLA corrections

1. Quark jet

In order to determine NMLLA corrections to the evolution Eq. (4), the 1-loop splitting functions (see [8]) are written as

$$\Phi_q^g(z) = C_F\left(\frac{2}{z} + \phi_q^g(z)\right),$$
$$(1-z)\Phi_g^g(z) = 2N_c\left(\frac{1}{z} + \phi_g^g(z)\right),$$

where $\phi_q^g(z) = (z-2)$ and $\phi_g^g(z) = (z-1)(2-z(1-z))$ are regular functions of z. The term proportional to $G(z)$ in the integrand of (4) becomes

$$\int_0^1 \mathrm{d}z \frac{\alpha_s}{\pi}\Phi_q^g(z)G(z) = 2C_F\int_0^1 \frac{\mathrm{d}z}{z}\frac{\alpha_s}{\pi}G(z) + C_F\int_0^1 \mathrm{d}z\frac{\alpha_s}{\pi}\phi_q^g(z)G(z), \quad (15)$$

the second part of which is expanded according to (13). Replacing $\alpha_s/\pi = \gamma_0^2/2N_c$ (see (9)), one gets

$$\int_0^1 \mathrm{d}z \frac{\alpha_s}{\pi}\Phi_q^g(z)G(z) \approx \frac{C_F}{N_c}\left[\left(\int_0^1 \frac{\mathrm{d}z}{z}\gamma_0^2 G(z)\right) - \frac{3}{4}\gamma_0^2 G + \frac{7}{8}\gamma_0^2 G_\ell + \ldots\right], \quad (16)$$

where $G_\ell \equiv G_\ell(1)$ and $Q_\ell \equiv Q_\ell(1)$. The first integral in the right-hand side of (16) provides the DLA (leading) term as $z \to 0$, while the second and third terms correspond to higher powers of $\sqrt{\alpha_s}$, that is MLLA and NMLLA corrections, respectively. The z-dependence of α_s in (16) has only been taken into account in the singular (DLA) part dominated by small z. On the contrary, for the nonsingular parts corresponding to branching processes in which $z \sim 1 - z = \mathcal{O}(1)$, α_s has been taken out of the z integral [18] as done in [5]. The dependence on the other variables, $k_\perp$, Θ, is of course unchanged.

Likewise, the term proportional to $Q(1-z) - Q$ in (4) can be expanded according to (13), leading to

$$\int_0^1 \mathrm{d}z \frac{\alpha_s}{\pi}\Phi_q^g(z)(Q(1-z) - Q) \approx \int_0^1 \mathrm{d}z \frac{\alpha_s}{\pi}Q_\ell\Phi_q^g(z)\ln(1-z) \approx \left(\frac{C_F}{N_c}\right)^2\gamma_0^2\left(\frac{5}{8} - \frac{\pi^2}{6}\right)G_\ell. \quad (17)$$

In the second line of (17), we have used the approximated formula $Q_\ell \approx C_F/N_c G_\ell + \mathcal{O}(\gamma_0^2)$ that holds at DLA because subleading terms would give $\mathcal{O}(\gamma_0^4)$ corrections which are beyond NMLLA (see also Appendix A). Finally, plugging (16) and (17) into (4), we obtain

$$Q_y = \frac{C_F}{N_c}\left\{\left(\int_0^1 \frac{\mathrm{d}z}{z}\gamma_0^2 G(z)\right) - \frac{3}{4}\gamma_0^2 G + \left[\frac{7}{8} + \frac{C_F}{N_c}\left(\frac{5}{8} - \frac{\pi^2}{6}\right)\right]\gamma_0^2 G_\ell\right\}, \quad (18)$$

where the term proportional to $\gamma_0^2 G_\ell = \mathcal{O}(\gamma_0^3)$ constitutes the new NMLLA correction. It is quite sizable and should be taken into account in the coming calculations.

2. Gluon jet

Along similar steps, we now evaluate NMLLA corrections to Eq. (5). The first term in the integral can be cast in the form

$$\int_0^1 \mathrm{d}z \frac{\alpha_s}{\pi}\Phi_g^g(z)(1-z)(G(z) + G(1-z) - G) \approx \left(\int_0^1 \frac{\mathrm{d}z}{z}\gamma_0^2 G(z)\right) - \frac{11}{12}\gamma_0^2 G + \left(\frac{67}{36} - \frac{\pi^2}{6}\right)\gamma_0^2 G_\ell, \quad (19)$$

and the second into

$$n_f\int_0^1 \mathrm{d}z \frac{\alpha_s}{\pi}\Phi_g^q(z)(2Q(z) - G) \approx \frac{2}{3}\frac{n_f T_R}{2N_c}\gamma_0^2(2Q - G) - \frac{13}{18}\frac{n_f T_R}{N_c}\gamma_0^2 Q_\ell. \quad (20)$$

Summing (19) and (20), replacing like before Q by its DLA formula $Q \approx C_F/N_c G$ (see Appendix A for further details), the evolution equation for particle spectra inside a gluon jet reads

$$G_y = \left(\int_0^1 \frac{\mathrm{d}z}{z}\gamma_0^2 G(z)\right) - \left[\frac{11}{12} + \frac{n_f T_R}{3N_c}\left(1 - 2\frac{C_F}{N_c}\right)\right]\gamma_0^2 G + \left(\frac{67}{36} - \frac{\pi^2}{6} - \frac{13}{18}\frac{n_f T_R}{N_c}\frac{C_F}{N_c}\right)\gamma_0^2 G_\ell. \quad (21)$$

The first term in parenthesis in (18) and (21) is, as stressed before, the main (double logarithmic) contribution. According to the Low-Barnett-Kroll theorem [19], the $\mathrm{d}z/z$ term, which is of classical origin, is universal, that is, independent of the process and of the partonic quantum numbers. The other two (single logarithmic) contributions,

which arise from hard parton splitting, are quantum corrections. It should also be noticed that, despite the large size of NMLLA corrections coming from $g \to gg$ and $g \to q\bar{q}$ splittings, a large cancellation occurs in their sum (21). The coefficients of the terms proportional to G_ℓ in (18) and in (21) are in agreement with [20].

3. NMLLA system of evolution equations

Once written in terms of $\ell' = \ln(z/x)$ and $y' = \ln(xE\Theta/Q_0)$, the system of two-coupled evolution Eqs. (18) and (21) finally reads

$$Q(\ell, y) = \delta(\ell) + \frac{C_F}{N_c}\int_0^\ell d\ell' \int_0^y dy' \gamma_0^2(\ell' + y') \times [1 - \tilde{a}_1\delta(\ell' - \ell) + \tilde{a}_2\delta(\ell' - \ell) \times \psi_\ell(\ell', y')]G(\ell', y'), \quad (22)$$

$$G(\ell, y) = \delta(\ell) + \int_0^\ell d\ell' \int_0^y dy' \gamma_0^2(\ell' + y')[1 - a_1\delta(\ell' - \ell) + a_2\delta(\ell' - \ell)\psi_\ell(\ell', y')]G(\ell', y'), \quad (23)$$

with $\psi_\ell \equiv G_\ell/G$ and the MLLA and NMLLA coefficients [21] given by

$$\tilde{a}_1 = \frac{3}{4}, \quad (24a)$$

$$a_1 = \frac{11}{12} + \frac{n_f T_R}{3N_c}\left(1 - 2\frac{C_F}{N_c}\right) \overset{n_f=3}{\approx} 0.935, \quad (24b)$$

$$\tilde{a}_2 = \frac{7}{8} + \frac{C_F}{N_c}\left(\frac{5}{8} - \frac{\pi^2}{6}\right) \approx 0.42, \quad (24c)$$

$$a_2 = \frac{67}{36} - \frac{\pi^2}{6} - \frac{13}{18}\frac{n_f T_R}{N_c}\frac{C_F}{N_c} \overset{n_f=3}{\approx} 0.06. \quad (24d)$$

As can be seen, the NMLLA coefficient a_2 is very small This may explain *a posteriori* why the MLLA "hump-backed plateau" agrees very well with experimental data [1,22]. Therefore, the NMLLA solution of (23) can be approximated by the MLLA solution of G (i.e. taking $a_2 = 0$), which will be used in the following to compute the inclusive $k_\perp$-distribution as well as 2-particle correlations inside a jet [23]. The MLLA gluon inclusive spectrum is given by [8]:

$$G(\ell, y) = 2\frac{\Gamma(B)}{\beta_0}\int_0^{\pi/2}\frac{d\tau}{\pi}e^{-B\alpha}\mathcal{F}_B(\tau, y, \ell), \quad (25)$$

where the integration is performed with respect to τ defined by $\alpha = \frac{1}{2}\ln\frac{y}{\ell} + i\tau$, and with

$$\mathcal{F}_B(\tau, y, \ell) = \left[\frac{\cosh\alpha - \frac{y-\ell}{y+\ell}\sinh\alpha}{\frac{\ell+y}{\beta_0}\frac{\alpha}{\sinh\alpha}}\right]^{B/2} I_B(2\sqrt{Z(\tau, y, \ell)}),$$

$$Z(\tau, y, \ell) = \frac{\ell + y}{\beta_0}\frac{\alpha}{\sinh\alpha}\left(\cosh\alpha - \frac{y - \ell}{y + \ell}\sinh\alpha\right),$$

$B = a_1/\beta_0$, and I_B is the modified Bessel function of the first kind. To get a quantitative idea on the difference between the MLLA and NMLLA gluon inclusive spectrum, the reader is referred to Appendix B where a simplified NMLLA equation (23) with a frozen coupling constant is solved. The magnitude of $\tilde{a}_2$, however, indicates that the NMLLA corrections to the inclusive quark jet spectrum may not be negligible and should be taken into account. After solving (23), the solution of (22) reads

$$Q(\ell, y) = \frac{C_F}{N_c}[G(\ell, y) + (a_1 - \tilde{a}_1)G_\ell(\ell, y) + (a_1(a_1 - \tilde{a}_1) + \tilde{a}_2 - a_2)G_{\ell\ell}(\ell, y)] + \mathcal{O}(\gamma_0^2). \quad (26)$$

It differs from the MLLA expression given in [4] by the term proportional to $G_{\ell\ell}$, which can be deduced from the subtraction of $(C_F/N_c) \times (23)$ to Eq. (22).

III. SINGLE-INCLUSIVE $k_\perp$-DISTRIBUTION IN THE LIMITING SPECTRUM

While MLLA calculations show that, asymptotically, the shape of the inclusive spectrum becomes independent of λ [8,24], setting the infrared cutoff Q_0 of cascading processes as low as the intrinsic QCD scale $\Lambda_{\rm QCD}$ is a daring hypothesis, since it is tantamount to assuming that a perturbative treatment can be trusted in regions of large running α_s. However, it turns out that, experimentally, this shape is very well described by $\lambda = 0$. We shall show below that this remarkable property is also true for the single-inclusive $k_\perp$-distribution. This will be further confirmed in Sec. IV in which nonvanishing values of λ are considered.

A. Double-differential distribution

The double-differential distribution $d^2N/(dx\,d\ln\theta)$ for the production of a single hadron h at angle Θ in a high-energy jet of total energy E and opening angle $\Theta_0 \geq \Theta$, carrying the energy-fraction x, is obtained by integrating the inclusive double-differential 2-particle cross section (see [4]) [25]. Then, the single-inclusive $k_\perp$-distribution of hadrons inside a jet is obtained by integrating $d^2N/(dx\,d\ln\theta)$ over all energy-fractions x:

$$\left(\frac{dN}{d\ln k_\perp}\right)_{q\text{ or }g} = \int dx\left(\frac{d^2N}{dx\,d\ln k_\perp}\right)_{q\text{ or }g} \equiv \int_{\ell_{\min}}^{Y_{\Theta_0}-y} d\ell\left(\frac{d^2N}{d\ell\,d\ln k_\perp}\right)_{q\text{ or }g}. \quad (27)$$

As in [4], a lower bound of integration, $\ell_{\min}$, is introduced since the present calculation is only valid in the small-x region, and therefore cannot be trusted when $\ell \equiv \ln(1/x)$ becomes "too" small. We shall discuss this in more detail in Sec. III C and Appendix G.

According to [4], $\frac{d^2N}{dx\,d\ln\Theta}$ can be expressed as

$$\frac{d^2N}{dx\,d\ln\Theta} = \frac{d}{d\ln\Theta} F^h_{\mathtt{A}_0}(x, \Theta, E, \Theta_0), \tag{28}$$

where $F^h_{\mathtt{A}_0}$, which represents the inclusive production of h in the subjet of opening angle Θ inside the jet A_0 of opening angle Θ_0, is given by a convolution product of two fragmentation functions [4]:

$$F^h_{\mathtt{A}_0}(x, \Theta, E, \Theta_0) \equiv \sum_{\mathtt{A}} \int_x^1 du D^{\mathtt{A}}_{\mathtt{A}_0}(u, E\Theta_0, uE\Theta) \times D^h_{\mathtt{A}}\left(\frac{x}{u}, uE\Theta, Q_0\right). \tag{29}$$

The convolution expresses the correlation between the energy flux of the jet and one particle within it. Equation (29) is schematically depicted in Fig. 2: u is the energy-fraction of the intermediate parton $\mathtt{A}$, $D^{\mathtt{A}}_{\mathtt{A}_0}$ describes the probability to emit $\mathtt{A}$ with energy uE off the parton $\mathtt{A}_0$ (which initiates the jet) taking into account the evolution of the jet between Θ_0 and Θ, and $D^h_{\mathtt{A}}$ describes the probability to produce the hadron h off $\mathtt{A}$ with energy-fraction x/u and transverse momentum $k_\perp \approx uE\Theta \geq Q_0$; $k_\perp$ is defined with respect to the jet axis which is, in this context, identified with the direction of the energy flux.

As discussed in [4], the convolution (29) is dominated by $u = \mathcal{O}(1)$. Therefore, $D^{\mathtt{A}}_{\mathtt{A}_0}(u, E\Theta_0, uE\Theta)$ is given by DGLAP evolution equations. On the contrary, since $x \ll u = \mathcal{O}(1)$ in the small-x limit where MLLA evolution equations are valid, $D^h_{\mathtt{A}}$ behaves as (see (10))

$$D^h_{\mathtt{A}}\left(\frac{x}{u}, uE\Theta, Q_0\right) \overset{x\ll u}{\approx} \frac{u}{x}\rho^h_{\mathtt{A}}\left(\ln\frac{u}{x}, \ln u + Y_\Theta\right). \tag{30}$$

Since $Y_\Theta + \ln u = \ell + \ln u + y$, the hump-backed plateau $\rho^h_{\mathtt{A}}$ depends on the two variables $\ell + \ln u$ and y, and we conveniently define $\tilde{D}$ as

$$\tilde{D}^h_{\mathtt{A}}(\ell + \ln u, y) \equiv \frac{x}{u} D^h_{\mathtt{A}}\left(\frac{x}{u}, uE\Theta, Q_0\right). \tag{31}$$

The Taylor expansion of $\rho^h_{\mathtt{A}}$ to the second order in $\ln u$ for $u \sim 1 \Leftrightarrow |\ln u| \ll 1$, that is, one step further than in [4], leads to

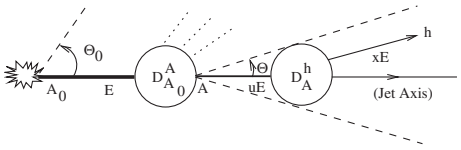

FIG. 2. Inclusive production of hadron h at an angle Θ inside a high-energy jet of total opening angle Θ_0.

$$xF^h_{\mathtt{A}_0}(x, \Theta, E, \Theta_0) \approx x\tilde{F}^h_{\mathtt{A}_0}(x, \Theta, E, \Theta_0) + \frac{1}{2}\sum_{\mathtt{A}}\left[\int du u(\ln^2 u) \times D^{\mathtt{A}}_{\mathtt{A}_0}(u, E\Theta_0, uE\Theta)\right]\frac{d^2\tilde{D}^h_{\mathtt{A}}(\ell, y)}{d\ell^2}, \tag{32}$$

where

$$x\tilde{F}^h_{\mathtt{A}_0}(x, \Theta, E, \Theta_0) \approx \sum_{\mathtt{A}}\left[\int du u(1 + (\ln u)\psi_{\mathtt{A},\ell}(\ell, y)) \times D^{\mathtt{A}}_{\mathtt{A}_0}(u, E\Theta_0, uE\Theta)\right]\tilde{D}^h_{\mathtt{A}}(\ell, y) \tag{33}$$

is the MLLA distribution calculated in [4]. In (33) we have introduced first logarithmic derivatives of $\tilde{D}^h_{\mathtt{A}}$:

$$\psi_{\mathtt{A},\ell}(\ell, y) = \frac{1}{\tilde{D}^h_{\mathtt{A}}(\ell, y)}\frac{d\tilde{D}_{\mathtt{A}}(\ell, y)}{d\ell} = \mathcal{O}(\sqrt{\alpha_s}). \tag{34}$$

Thus, as in [4], in the soft limit the correlation disappears and the convolution (29) is reduced to the factorized expression in (32).

The second term in the right-hand side of (32) is the new NMLLA correction calculated in this paper. Since x/u is small, the inclusive spectrum $\tilde{D}^h_{\mathtt{A}}(\ell, y)$ occurring in (32) should be taken as the next-to-MLLA solution of the evolution Eqs. (22) and (23). However, as already mentioned and shown in Appendix B, the MLLA inclusive spectrum for a gluon jet can be used as a good approximation for (23) (with $a_1 \neq 0$, $a_2 = 0$) such that, in (33), it is enough to use this level of approximation. So, we shall therefore use Eqs. (25) and (26) in the following.

The NMLLA correction in (32) globally decreases $|xF^h_{\mathtt{A}_0}|$ in the perturbative region ($y \geq 1.5$). Indeed, while the MLLA part proportional to $\ln u$ in (33) is negative [4], it is instead, there, positive because of the positivity of u and $\ln^2 u$ and $\frac{d^2\tilde{D}^h_{\mathtt{A}}}{d\ell^2} \simeq \frac{d^2G}{d\ell^2}$ (see Fig. 18 in Appendix C). The NMLLA contribution therefore tempers somehow the size of the MLLA corrections when y is large enough.

B. Color currents

The function $F^h_{\mathtt{A}_0}$ is related to the inclusive gluon distribution *via* the color currents defined as [4,8]

$$xF^h_{\mathtt{A}_0} = \frac{\langle C\rangle_{\mathtt{A}_0}}{N_c} G(\ell, y). \tag{35}$$

The color current can be seen as the average color charge carried by the parton $\mathtt{A}$ due to the DGLAP evolution from $\mathtt{A}_0$ to $\mathtt{A}$. Introducing the first and second logarithmic derivatives of $\tilde{D}^h_{\mathtt{A}}$,

$$(\psi^2_{\mathrm{A},\ell} + \psi_{\mathrm{A},\ell\ell})(\ell, y) = \frac{1}{\tilde{D}^h_{\mathrm{A}}(\ell, y)} \frac{\mathrm{d}^2 \tilde{D}_{\mathrm{A}}(\ell, y)}{\mathrm{d}\ell^2} = \mathcal{O}(\alpha_s), \tag{36}$$

which are MLLA and NMLLA corrections, respectively, Eq. (32) can now be written as

$$xF^h_{\mathrm{A}_0} \approx \sum_{\mathrm{A}} \Big[\langle u \rangle^{\mathrm{A}}_{\mathrm{A}_0} + \langle u \ln u \rangle^{\mathrm{A}}_{\mathrm{A}_0} \psi_{\mathrm{A},\ell}(\ell, y) + \frac{1}{2} \langle u \ln^2 u \rangle^{\mathrm{A}}_{\mathrm{A}_0} (\psi^2_{\mathrm{A},\ell} + \psi_{A,\ell\ell})(\ell, y) \Big] \tilde{D}^h_{\mathrm{A}}(\ell, y),$$

where

$$\langle u \ln^i u \rangle^{\mathrm{A}}_{\mathrm{A}_0} \equiv \int_0^1 \mathrm{d}u (u \ln^i u) D^{\mathrm{A}}_{\mathrm{A}_0}(u, E\Theta_0, uE\Theta). \tag{37}$$

Unlike in [4] at MLLA, using the approximation $u = \mathcal{O}(1)$ to replace in (37) $uE\Theta$ by $E\Theta$ requires here some care, since the resulting scaling violation of the DGLAP fragmentation functions also provides $\mathcal{O}(\alpha_s)$ corrections to $\langle u \rangle$. Explicit calculations (see Appendix D) show that they never exceed 5% of the leading term. Accordingly, we neglect them in the following and replace (37) by

$$\langle u \ln^i u \rangle^{\mathrm{A}}_{\mathrm{A}_0} \simeq \int_0^1 \mathrm{d}u (u \ln^i u) D^{\mathrm{A}}_{\mathrm{A}_0}(u, E\Theta_0, E\Theta). \tag{38}$$

The total average color current $\langle C \rangle_{\mathrm{A}_0}$ of partons caught by the calorimeter decomposes accordingly into three terms which can be written as

$$\langle C \rangle_{\mathrm{A}_0} = \langle C \rangle^{\mathrm{LO}}_{\mathrm{A}_0} + \delta \langle C \rangle^{\mathrm{MLLA-LO}}_{\mathrm{A}_0} + \delta \langle C \rangle^{\mathrm{NMLLA-MLLA}}_{\mathrm{A}_0}. \tag{39}$$

The leading order (LO) $\mathcal{O}(1)$ and MLLA $\mathcal{O}(\sqrt{\alpha_s})$ contributions to the color currents have been determined in [4]. The new NMLLA $\mathcal{O}(\alpha_s)$ correction evaluated in this paper reads

$$\delta \langle C \rangle^{\mathrm{NMLLA-MLLA}}_{\mathrm{A}_0} = N_c \langle u \ln^2 u \rangle^g_{\mathrm{A}_0} (\psi^2_{g,\ell} + \psi_{g,\ell\ell}) + C_F \langle u \ln^2 u \rangle^q_{\mathrm{A}_0} (\psi^2_{q,\ell} + \psi_{q,\ell\ell}), \tag{40}$$

assuming $Q = C_F/N_c G$. We checked that using instead the NMLLA exact formula (26) for the quark inclusive spectrum Q actually leads to negligible corrections to the color currents (see Appendix E). Equation (40) can be obtained from the Mellin-transformed DGLAP fragmentation functions

$$\mathcal{D}^{\mathrm{A}}_{\mathrm{A}_0}(j, \xi) = \int_0^1 \mathrm{d}u u^{j-1} D^{\mathrm{A}}_{\mathrm{A}_0}(u, \xi),$$

through the formula

$$\langle u \ln^2 u \rangle^{\mathrm{A}}_{\mathrm{A}_0} = \frac{\mathrm{d}^2}{\mathrm{d}j^2} \mathcal{D}^{\mathrm{A}}_{\mathrm{A}_0}(j, \xi(E\Theta_0) - \xi(E\Theta))|_{j=2} \equiv \int_0^1 \mathrm{d}u u \ln^2 u D^{\mathrm{A}}_{\mathrm{A}_0}(u, \xi). \tag{41}$$

Given the rather lengthy expressions, the complete analytic results for $\langle C \rangle^{\mathrm{NMLLA-MLLA}}_{\mathrm{A}_0}$ for quark and gluon jets are given in Appendix F.

For illustrative purposes, the color currents are plotted in Fig. 3 in the limiting spectrum approximation ($\lambda = 0$). The LO (solid line), MLLA (dash-dotted) and NMLLA (dashed) currents are computed for a quark (top) and for a gluon jet (bottom) with energy $Y_{\Theta_0} = 6.4$—corresponding to Tevatron energies—and at fixed $\ell = 2$. As can be seen in Fig. 3, NMLLA $\mathcal{O}(\alpha_s)$ corrections to the MLLA color currents are clearly not negligible, yet of course somewhat smaller than the MLLA $\mathcal{O}(\sqrt{\alpha_s})$ corrections to the LO result. In the perturbative region ($y > 1.5$), these corrections are positive and consequently decrease the difference with the LO estimate. On the contrary, at small $y \leq 1.5$, the corrections are rather large and negative coming from the negative sign of $G_{\ell\ell}(\ell, y)$ (see Fig. 18 in

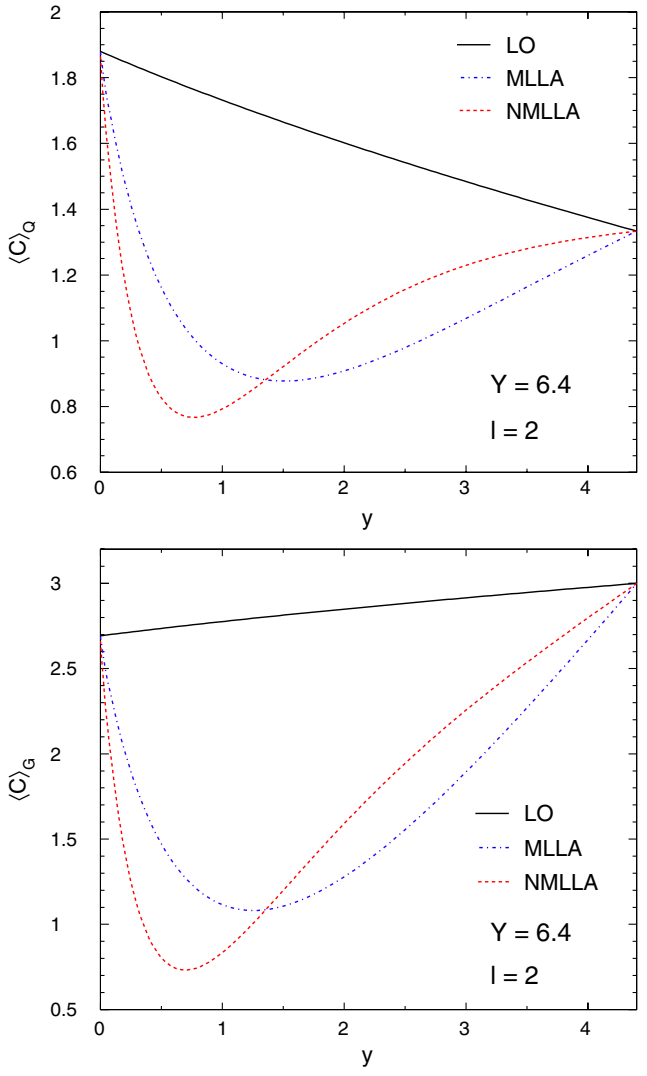

FIG. 3 (color online). Color currents at LO (solid lines), MLLA (dash-dotted), and NMLLA (dashed) for a quark (top) and gluon jet (bottom) with $Y_{\Theta_0} = 6.4$ and $\ell = 2$.

Appendix C). However, it should be kept in mind that as y goes to 0, $k_\perp$ gets closer to $\Lambda_{\rm QCD}$ (recall that $Q_0 = \Lambda_{\rm QCD}$ in the limiting spectrum approximation) and, thus, the present perturbative predictions may not be reliable in this domain.

Note also that both the MLLA and NMLLA corrections vanish at $y = 0$ (since $G_\ell = G_{\ell\ell} = 0$) and when $\Theta = \Theta_0$. Another interesting property to mention is the decrease of MLLA and NMLLA corrections as ℓ increases, that is, when partons get softer and recoil effects more negligible.

From the color currents, the NMLLA double-differential 1-particle distribution at small x (see Eq. (28)),

$$\left(\frac{\mathrm{d}^2N}{\mathrm{d}\ell\mathrm{d}y}\right)_{\mathbb{A}_0} = \frac{1}{N_c}\langle C\rangle_{\mathbb{A}_0}\frac{\mathrm{d}}{\mathrm{d}y}G(\ell, y) + \frac{1}{N_c}G(\ell, y)\frac{\mathrm{d}}{\mathrm{d}y}\langle C\rangle_{\mathbb{A}_0}, \tag{42}$$

can be determined for any value of λ. The NMLLA behavior of $\mathrm{d}^2N/\mathrm{d}\ell\mathrm{d}y$ is therefore easily deduced from $\langle C\rangle_{\mathbb{A}_0}$ and its y-dependence, $\mathrm{d}\langle C\rangle_{\mathbb{A}_0}/\mathrm{d}y$.

C. $k_\perp$-distributions

The $k_\perp$-distributions of hadrons are computed from the numerical integration of the double-differential cross section, Eq. (42). On Fig. 4 are shown the MLLA (dashed lines) and NMLLA (solid lines) $\mathrm{d}N/\mathrm{d}y$ distributions for a quark (left) and a gluon jet (right) with $Y_{\Theta_0} = 4.3$ and $Y_{\Theta_0} = 6.4$.

The size of NMLLA corrections proves quite substantial over the whole y-range. We find, in particular, that at large y (or $k_\perp$), the distributions at NMLLA are lower than at MLLA (and larger at small y). This softening of the spectra can be understood physically by the role of energy conservation in jets. With respect to DLA, MLLA and NMLLA take better into account the recoil of the emitting parton at each step of the cascading process. The fraction of energy carried away by the emitted soft partons gets reduced, which finally damps the final emission of hadrons at large $k_\perp$ [26]. As already stressed in Sec. III A, the value of the lower limit of integration $\ell_{\rm min}$ below which the present small-x calculation may not be trusted cannot be directly predicted. In [4], the appearance of positivity problems in the double-differential distribution at small ℓ led us to consider a minimal value $\ell_{\rm min}$ such that $\mathrm{d}^2N/\mathrm{d}\ell\mathrm{d}\ln k_\perp$ is kept positive for all $\ell \geq \ell_{\rm min}$, leading to [27] $\ell_{\rm min} \simeq 2.5$. For consistency, the same criterion is used in the present paper. We find that smaller values of ℓ actually fulfill the positivity requirement, roughly $\ell_{\rm min} \simeq 2$ and $\ell_{\rm min} \simeq 1$ for quark and gluon jets at Tevatron energies.

It is interesting to note that the range over which NMLLA calculations appear sensible extends to smaller ℓ, therefore to larger x, than at MLLA; this also corresponds to larger y at fixed Y. One could therefore expect the present NMLLA predictions to agree with experimental results in a larger domain of $k_\perp$. This is discussed in the coming section.

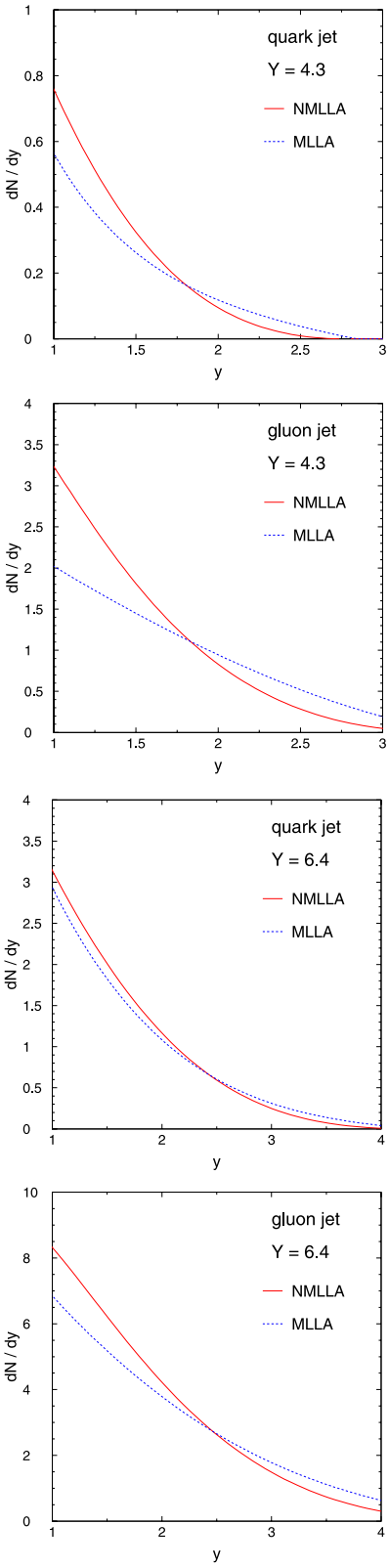

FIG. 4 (color online). MLLA (dashed lines) and NMLLA (solid lines) inclusive y-distributions. From top to bottom: 2 upper pictures: quark then gluon jet at $Y_{\Theta_0} = 4.3$ ($Q = 19$ GeV); 2 lower pictures: quark then gluon jet at $Y_{\Theta_0} = 6.4$ ($Q = 155$ GeV).

D. Comparison with CDF preliminary data

The CDF Collaboration at Tevatron recently reported on preliminary data of hadronic single-inclusive $k_\perp$-distributions inside jets produced in $p\bar{p}$ collisions at $\sqrt{s} = 1.96$ TeV [7]. The measurements cover a wide domain of jet energies, with hardness $Q = E\Theta_0$ ranging from $Q = 19$ GeV to $Q = 155$ GeV. The CDF results, including systematic errors, are plotted in Fig. 5 together with the MLLA predictions of [4] (dashed lines) and the present NMLLA calculations (solid lines). Data and theory are normalized to the same bin, $\ln k_\perp = -0.1$, because of presently too large normalization errors in the CDF preliminary data. The experimental measurements reflect a mixing of quark and gluon jets:

$$\left(\frac{\mathrm{d}N}{\mathrm{d}\ln k_\perp}\right)_{\mathrm{mix}} = \omega\left(\frac{\mathrm{d}N}{\mathrm{d}\ln k_\perp}\right)_g + (1-\omega)\left(\frac{\mathrm{d}N}{\mathrm{d}\ln k_\perp}\right)_q \qquad (43)$$

characterized by one Q-dependent mixing-parameter ω, estimated from PYTHIA [28], used in the theoretical calculation.

The agreement between the CDF results and the NMLLA distributions over the whole $k_\perp$-range is excellent. The NMLLA calculation is, in particular, able to capture the shape of CDF spectra at all Q. Conversely, predictions at MLLA prove only reliable at not too large $k_\perp$.

The domain of validity of the predictions has been enlarged to larger $k_\perp$ (and thus to larger x since Y is fixed) computing from MLLA to NMLLA accuracy [29]. However, it should be mentioned that, due to the normalization at the first bin, this extension of the domain of prediction only concerns, strictly speaking, the shape of the distribution. Equally important, the agreement between NMLLA calculations and experimental results brings further support to the Local Parton Hadron Duality (LPHD) picture [3]. We indeed find it remarkable to observe that the entire $k_\perp$-domain probed experimentally can be very well described by strict perturbation theory, leaving out only limited nonperturbative dynamics in the production of hadrons inside a jet, at least for inclusive enough observable like single-particle $k_\perp$-distributions.

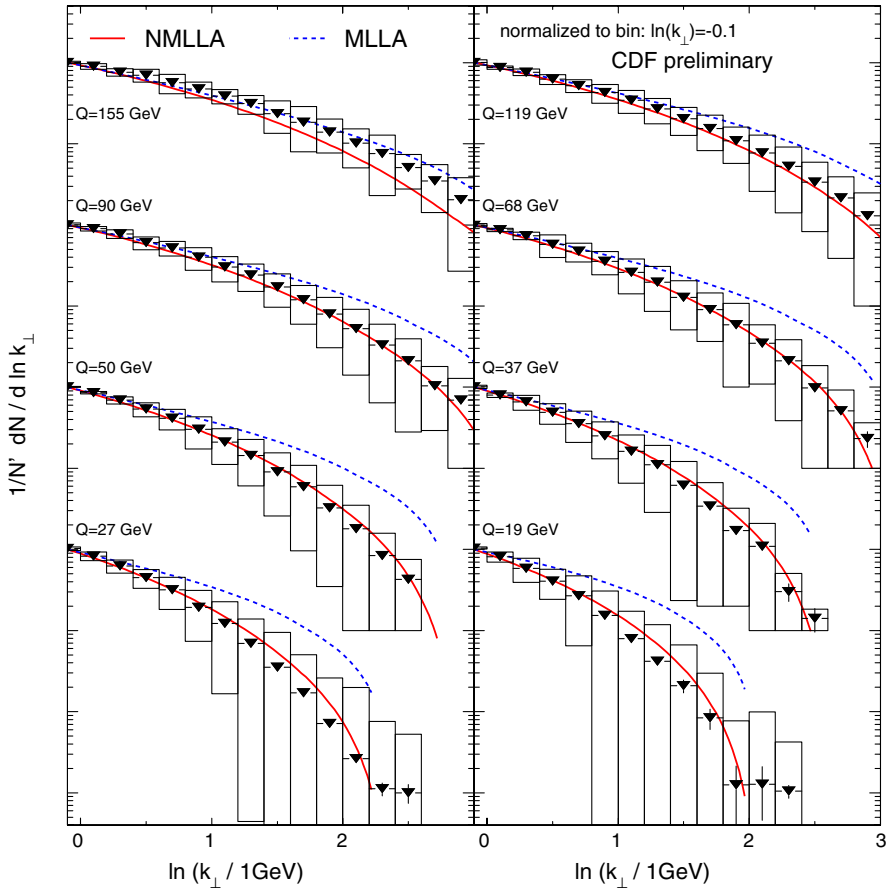

FIG. 5 (color online). CDF preliminary results on hadronic single-inclusive $k_\perp$-distributions, compared with MLLA (dashed lines) and NMLLA (solid lines) calculations at the limiting spectrum; the boxes are the systematic errors (their lower limits are cut at large $k_\perp$ for the sake of clarity).

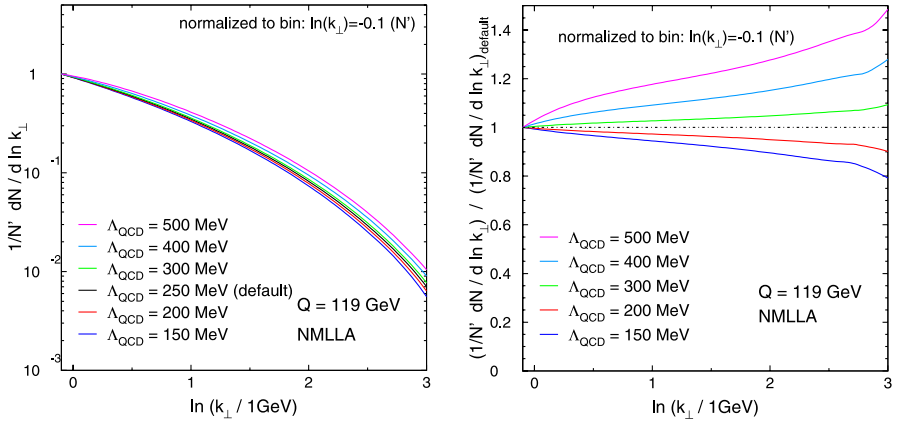

FIG. 6 (color online). The dependence on $\Lambda_{\rm QCD}$, absolute (left) and relative (right). The curves and the values of $\Lambda_{\rm QCD}$ indicated in the caption are set in the same order.

E. Theoretical uncertainties

The spectacular agreement between our NMLLA calculations and preliminary data should not hide the theoretical uncertainties that affect the former.

First, we did not take into account all NMLLA corrections. While scaling violations have already been dealt with in Sec. III B and Appendix D, other NMLLA corrections arise from varying $\Lambda_{\rm QCD}$ in the expression of α_s. In Figs. 6 the inclusive $k_\perp$-distribution ($Q = 119$ GeV) is plotted at values of $\Lambda_{\rm QCD}$ ranging from 150 to 500 MeV (left), as well as the ratio to its value at the default $\Lambda_{\rm QCD} =$ 250 MeV (right). All curves have been normalized to the bin $\ln(k_\perp/1\ {\rm GeV}) = -0.1$. In the largest bin $\ln(k_\perp/1\ {\rm GeV}) = 3$, varying $\Lambda_{\rm QCD}$ ranging from 150 to 400 MeV does not yield a relative variation larger than 20%. The corresponding curves still fall within the experimental systematic errors. Note that the fact that variations seem only important at large $k_\perp$ only comes from the normalization procedure in the bin $\ln(k_\perp/1\,{\rm GeV}) = -0.1$. A more delicate matter concerns the dominance of the type of NMLLA corrections that we have taken into account. Some remarks concerning this point are postponed to the general discussion in Sec. VI.

The second point concerns the jet axis, which is defined here as the direction of the energy flow. It is implicitly determined by a summation over all secondary hadrons in energy-energy correlations. At the opposite, the jet axis is experimentally determined exclusively from *all* particles inside the jet. Whether these two definitions match within NMLLA accuracy, $\mathcal{O}(\alpha_s)$, is a matter which deserves further investigation. This goes however beyond the scope of the present work.

Last, cutting the integral (27) at small ℓ may look somewhat arbitrary. However, at the end of Appendix G, we provide curves which show the variation of the inclusive $k_\perp$-distribution at MLLA and NMLLA when $\ell^g_{\rm min}$ is changed. Varying it from 1 to 1.75 does not modify the NMLLA spectrum at large $k_\perp$ by more than 20%. Variations are more dramatic at MLLA.

IV. SINGLE-INCLUSIVE $k_\perp$-DISTRIBUTIONS BEYOND THE LIMITING SPECTRUM

A. Inclusive spectrum

So far, the calculations have been performed in the limiting spectrum approximation, $Q_0 = \Lambda_{\rm QCD}$ or $\lambda = 0$. This assumption, which cuts off hadronic yield below Q_0, should be valid as long as the mass of the produced hadrons is not too large as compared to $\Lambda_{\rm QCD}$. This is the case when dealing mostly with pions. We perform in this section the exact calculation of single-inclusive spectra as well as $k_\perp$-distributions beyond this approximation, $\lambda \neq 0$, that is for hadrons with mass $m_h \simeq Q_0 \neq \Lambda_{\rm QCD}$ [24].

The inclusive gluon spectrum was given in [5] a compact Mellin representation:

$$G(\ell, y) = (\ell + y + \lambda) \int \frac{{\rm d}\omega {\rm d}\nu}{(2\pi i)^2} e^{\omega\ell + \nu y} \int_0^\infty \frac{{\rm d}s}{\nu + s} \times \left(\frac{\omega(\nu + s)}{(\omega + s)\nu}\right)^{1/\beta_0(\omega-\nu)} \left(\frac{\nu}{\nu + s}\right)^{a_1/\beta_0} e^{-\lambda s},$$

from which an analytic approximated expression was found using the steepest descent method [6]. However, $G(\ell, y)$ is here determined exactly from an equivalent representation in terms of a single Mellin transform (which reduces to (25) as $\lambda \to 0$) [24]

$$G(\ell, y) = \frac{\ell + y + \lambda}{\beta_0 B(B+1)} \int_{\epsilon - i\infty}^{\epsilon + i\infty} \frac{{\rm d}\omega}{2\pi i} e^{\omega\ell} \Phi(-A + B + 1, B + 2, -\omega(\ell + y + \lambda)) \mathcal{K}(\omega, \lambda) \quad (44)$$

which is better suited for numerical studies. The function $\mathcal{K}$ appearing in Eq. (44) reads

$$\mathcal{K}(\omega, \lambda) = \frac{\Gamma(A)}{\Gamma(B)} (\omega\lambda)^B \Psi(A, B + 1, \omega\lambda), \quad (45)$$

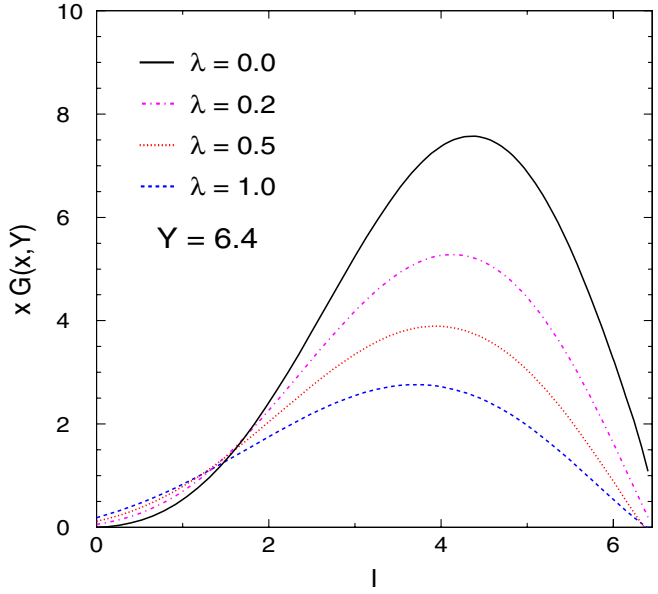

FIG. 7 (color online). Inclusive spectrum for a gluon jet ($Y_{\Theta_0} = 6.4$) for different values of λ.

where $A = 1/(\beta_0\omega)$, $B = a_1/\beta_0$, and Φ and Ψ are the confluent hypergeometric function of the first and second kind, respectively. The single-inclusive spectrum at MLLA is plotted in Fig. 7 for various values of λ, $\lambda = 0$, 0.2, 0.5, 1, for a gluon jet with $Y_\Theta = 6.4$. Increasing λ reduces the emission in the infrared region and therefore favors hard particle production at $\ell \ll Y/2$ (asymptotic position of the peak of the hump-backed plateau). Still, it is worth remarking that the global shape of G at finite λ remains similar to that obtained in the limiting spectrum approximation. Note also that there is a discrete part at finite λ, proportional to $\delta(\ell)$, corresponding to the finite probability for no parton emission when $Q_0 \neq \Lambda_{\rm QCD}$, the parton multiplicity becoming infrared finite at $\lambda \neq 0$ (see the second reference in [24]).

B. Color currents

The color currents, Eq. (39), can now be determined beyond the limiting spectrum from the inclusive spectrum calculated in the previous section. In Fig. 8 are displayed the MLLA corrections to the LO color current, $\delta\langle C\rangle^{\rm MLLA-LO}_{\tilde{A}_0}/\langle C\rangle^{\rm LO}_{\tilde{A}_0}$ (top), and NMLLA corrections to the MLLA color currents, $\delta\langle C\rangle^{\rm NMLLA-MLLA}_{\tilde{A}_0}/\langle C\rangle^{\rm MLLA}_{\tilde{A}_0}$ (bottom), for different values $\lambda = 0$, 0.5, 1. Figure 8 clearly indicates that the larger the values of λ, the smaller the MLLA (and NMLLA) corrections. In particular, MLLA (NMLLA) corrections can be as large as 50% (30%) in the limiting spectrum but no more than 20% (10%) for $\lambda = 1$. This is not surprising since $\lambda \neq 0$ ($Q_0 \neq \Lambda_{\rm QCD}$) reduces the parton emission in the infrared sector and, consequently, higher-order corrections.

As discussed in Sec. III B, the large and negative corrections to the color currents in the limiting spectrum lead

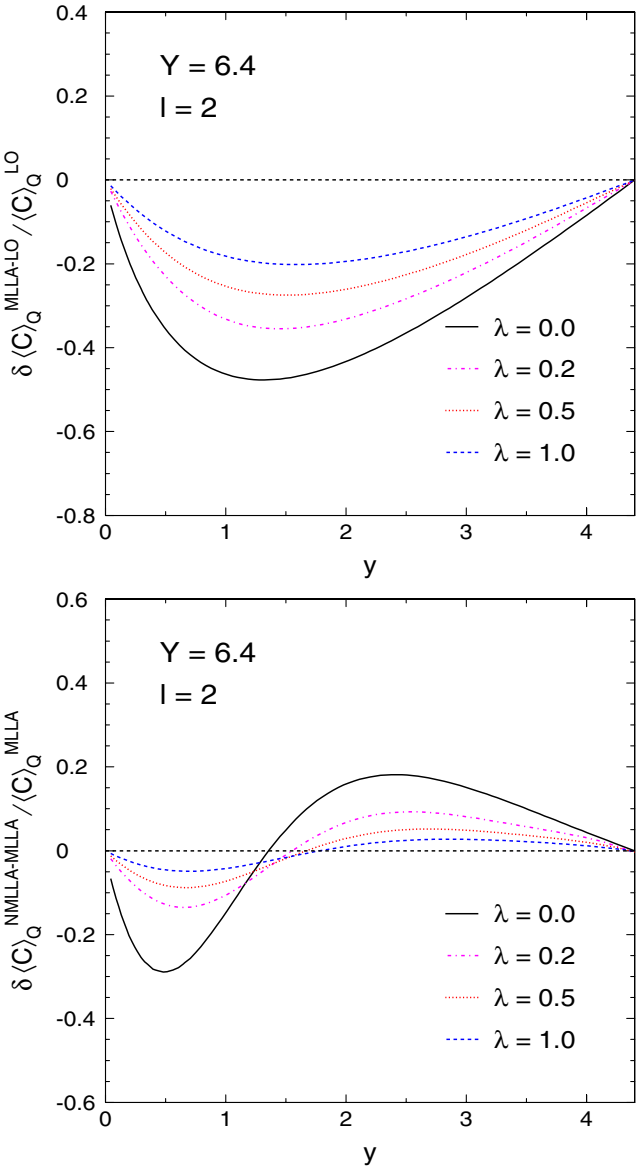

FIG. 8 (color online). MLLA (top) and NMLLA (bottom) normalized corrections to the LO and MLLA color currents, respectively, for different values of λ.

to negative double-differential spectra, $d^2N/d\ell dy$ at small y. Interestingly, at $\lambda \neq 0$, the infrared sensitivity is somehow weakened. As a consequence, $d^2N/d\ell dy$ is no longer negative at finite λ, as illustrated in Fig. 9. Another interesting consequence is the disappearance of the infrared divergence at $y = 0$ in the limiting spectrum, coming from the running of α_s: since $Q_0 \neq \Lambda_{\rm QCD}$, α_s and therefore $d^2N/d\ell dy$ remain finite over the full momentum-space.

C. $k_\perp$-distributions

The absolute $k_\perp$-distributions of "massive" hadrons is computed in Fig. 10 (top) for various values of λ for jets with hardness $Q = 119$ GeV. As expected, as λ gets

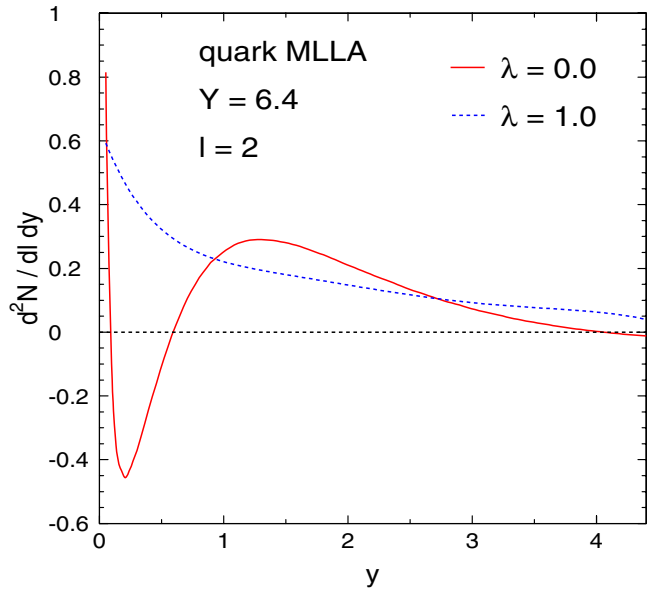

FIG. 9 (color online). MLLA double-differential distribution for a quark jet $Y_{\Theta_0} = 6.4$ computed at $\lambda = 0$ (solid line) and $\lambda = 1$ (dashed line).

larger, soft gluon emission is strongly suppressed such that the distribution flattens at small $k_\perp$, while more hadrons are produced at large $k_\perp$, making in turn the distributions harder. We also compare in Fig. 10 (bottom) these calculations with CDF preliminary data, all normalized to the $\log(k_\perp/1\ \mathrm{GeV}) = -0.1$ bin as before. The best description is reached in the limiting spectrum approximation, or at least for small values of $\lambda \lesssim 0.5$. This is not too surprising since these inclusive measurements mostly involve pions.

Predictions beyond the limiting spectrum were shown to describe very well the hump-backed shape of the inclusive spectra for various hadron species; in particular, the hadron-mass variation of the peak turned out to be in good agreement with QCD expectations (see e.g. [2]). The softening of the $k_\perp$-spectra with increasing hadron masses predicted in Fig. 10 is an observable worth to be measured, as this would provide an additional and independent check of the LPHD hypothesis beyond the limiting spectrum. This could only be achieved if the various species of hadrons inside a jet can be identified experimentally. Fortunately, it is likely to be the case at the LHC, where the ALICE [30] and CMS [31] experiments at the Large Hadron Collider have good identification capabilities at not too large transverse momenta.

V. 2-PARTICLE CORRELATIONS

A. Correlators and evolution equations

We work, like in [5], with the normalized correlators

$$\mathcal{C}_g = \frac{G^{(2)}}{G_1 G_2}, \qquad \mathcal{C}_q = \frac{Q^{(2)}}{Q_1 Q_2} \tag{46}$$

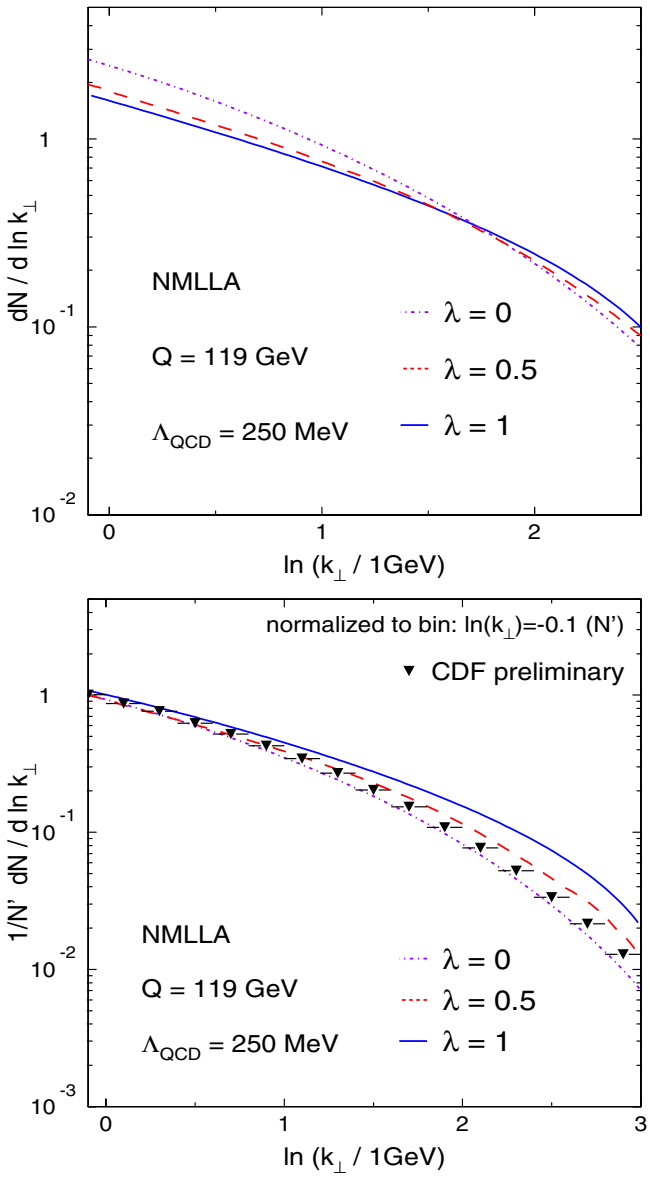

FIG. 10 (color online). Absolute (top) and normalized (bottom) inclusive $k_\perp$-distribution beyond the limiting spectrum approximation at NMLLA in a jet of hardness $Q = 119$ GeV.

where G_i, Q_i, $i = 1, 2$ are the inclusive spectra relative to the outgoing hadrons h_1 and h_2, and $G^{(2)}$, $Q^{(2)}$ are the 2-particle distributions in gluon and quark jets, respectively. The former are obtained by a single differentiation of the "MLLA" generating functional Z, and the latter by differentiating it twice [5] (see also the discussion introduced in Sec. II). Z satisfies the evolution equation described in Sec. (2) of [5]: $\mathrm{d}Z_{\mathtt{A}}/\mathrm{d}\ln\Theta$ for the jet initiating parton $\mathtt{A}$ is expressed as an integral over z involving the DGLAP splitting functions $\Phi_{\mathtt{A}}^{\mathtt{BC}}(z)$ and $Z_{\mathtt{B}}$ and $Z_{\mathtt{C}}$ associated to the products $\mathtt{B}$ and $\mathtt{C}$ of the splitting process; $\mathtt{B}$ carries away the fraction z of the energy E of $\mathtt{A}$ and $\mathtt{C}$ the fraction $(1 - z)$ (see Fig. 11). The topology of Fig. 11 respects the exact

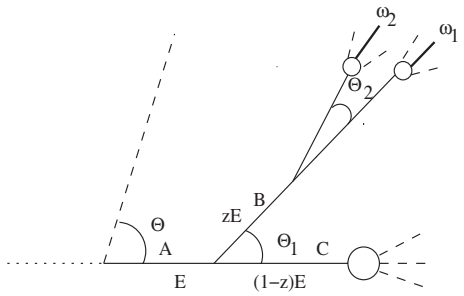

FIG. 11. 2-particle correlations inside a jet.

AO constraint over the successive emission angles of partons ($\Theta \geq \Theta_1 \geq \Theta_2$).

In practice, suitably differentiating the master evolution equation for $Z_{\mathbb{A}}$, which arises as a consequence of exact AO in parton cascades, yields, for the *correlation functions* [8]

$$\begin{aligned} G^{(2)} - G_1 G_2 &\equiv (\mathcal{C}_g - 1) G_1 G_2, \\ Q^{(2)} - Q_1 Q_2 &\equiv (\mathcal{C}_q - 1) Q_1 Q_2, \end{aligned} \tag{47}$$

the system of coupled evolution equations:

$$\begin{aligned} (Q^{(2)} - Q_1 Q_2)_y = \int_0^1 \mathrm{d}z \frac{\alpha_s}{\pi} \Phi_q^g(z) [G^{(2)}(z) + (Q^{(2)}(1-z) \\ - Q^{(2)}) + (G_1(z) - Q_1)(Q_2(1-z) \\ - Q_2) + (G_2(z) - Q_2)(Q_1(1-z) \\ - Q_1)], \end{aligned} \tag{48}$$

$$\begin{aligned} (G^{(2)} - G_1 G_2)_y = \int_0^1 \mathrm{d}z \frac{\alpha_s}{\pi} \Phi_g^g(z) [(G^{(2)}(z) - z G^{(2)}) \\ + (G_1(z) - G_1)(G_2(1-z) - G_2)] \\ + \int_0^1 \mathrm{d}z \frac{\alpha_s}{\pi} n_f \Phi_g^q(z) [2(Q^{(2)}(z) \\ - Q_1(z) Q_2(z)) - (G^{(2)} - G_1 G_2) \\ + (2Q_1(z) - G_1)(2Q_2(1-z) - G_2)]. \end{aligned} \tag{49}$$

The derivative is taken with respect to $y = Y - \ell$ rather than with respect to $\ln\Theta$, since it is more convenient when a collinear cutoff is imposed (see Sec. (2.1) of [5]). Like for the inclusive spectra, the notations have been lightened to a maximum, with $G^{(2)}$ standing for $G^{(2)}(z=1)$ and likewise for $Q^{(2)}$. The notation $x_i, \ell_i, \ldots$ refers to the $\ell_i = \ln(1/x_i)$ of the outgoing parton (hadron) i.

B. Including NMLLA corrections

We follow the same logic, exposed in Sec. II C, for the 2-particle distributions $Q^{(2)}$, $G^{(2)}$, as the one used for the inclusive spectra B in Sec. III A. Therefore, the expansion at small x_1, x_2 is performed for $\frac{x_1}{z} Q_1(\frac{x_1}{z}) \frac{x_2}{z} Q_2(\frac{x_2}{z})$ and $\frac{x_1}{z} G_1(\frac{x_1}{z}) \frac{x_2}{z} G_2(\frac{x_2}{z})$ as well as for $\frac{x_1}{z} \frac{x_2}{z} Q^{(2)}(\frac{x_1}{z}, \frac{x_2}{z})$ and $\frac{x_1}{z} \times \frac{x_2}{x} G^{(2)}(\frac{x_1}{z}, \frac{x_2}{z})$, similarly to Eq. (11).

1. Quark jet

Operating like for (16) and (17), the first (MLLA) term in the right-hand side of (48) can be cast in the form

$$\begin{aligned} \int_0^1 \mathrm{d}z \frac{\alpha_s}{\pi} \Phi_q^g(z) [G^{(2)}(z) + (Q^{(2)}(1-z) - Q^{(2)})] \\ = \frac{C_F}{N_c} \left[\int_0^1 \frac{\mathrm{d}z}{z} \gamma_0^2 G^{(2)}(z) \right] - \frac{3}{4} \frac{C_F}{N_c} \gamma_0^2 G^{(2)} \\ + \frac{C_F}{N_c} \left[\frac{7}{8} + \frac{C_F}{N_c} \left(\frac{5}{8} - \frac{\pi^2}{6} \right) \right] \gamma_0^2 G_\ell^{(2)} \\ + \left(\frac{C_F}{N_c} \right)^2 \left(\frac{C_F}{N_c} - 1 \right) \left(\frac{5}{8} - \frac{\pi^2}{6} \right) \gamma_0^2 (G_1 G_2)_\ell, \end{aligned} \tag{50}$$

where we have plugged the DLA formula [22]

$$Q_\ell^{(2)} = \frac{C_F}{N_c} G_\ell^{(2)} + \frac{C_F}{N_c} \left(\frac{C_F}{N_c} - 1 \right) (G_1 G_2)_\ell + \mathcal{O}(\gamma_0^2) \tag{51}$$

in the right-hand side of (50); the terms in (51) of relative order $\mathcal{O}(\gamma_0)$ are neglected because their contribution provides corrections to (50) beyond NMLLA (see also Appendix H). The second and third terms in the right-hand side of (48) provide the NMLLA correction:

$$\begin{aligned} \int_0^1 \mathrm{d}z \frac{\alpha_s}{\pi} \Phi_q^g(z) (G_1(z) - Q_1)(Q_2(1-z) - Q_2) \\ = \frac{\alpha_s}{\pi} \left(\int_0^1 \mathrm{d}z \Phi_q^g(z) \ln(1-z) \right) (G_1 - Q_1) Q_{2,\ell} \\ = \left(\frac{C_F}{N_c} \right)^2 \left(1 - \frac{C_F}{N_c} \right) \left(\frac{5}{8} - \frac{\pi^2}{6} \right) \gamma_0^2 G_1 G_{2,\ell}, \end{aligned} \tag{52}$$

where the DLA expression $Q_\ell = \frac{C_F}{N_c} G_\ell + \mathcal{O}(\gamma_0^2)$ is used [22]; further corrections ($\mathcal{O}(\gamma_0^2)$) to this formula are here again dropped out because their inclusion goes beyond the present resummation logic. Likewise, we have

$$\begin{aligned} \int_0^1 \mathrm{d}z \frac{\alpha_s}{\pi} \Phi_q^g(z) (G_2(z) - Q_2)(Q_1(1-z) - Q_1) \\ = \left(\frac{C_F}{N_c} \right)^2 \left(1 - \frac{C_F}{N_c} \right) \left(\frac{5}{8} - \frac{\pi^2}{6} \right) \gamma_0^2 G_{1,\ell} G_2. \end{aligned} \tag{53}$$

Gathering (50), (52), and (53) yields

$$\begin{aligned} (Q^{(2)} - Q_1 Q_2)_y = \frac{C_F}{N_c} \left[\int_0^1 \frac{\mathrm{d}z}{z} \gamma_0^2 G^{(2)}(z) \right] - \frac{3}{4} \frac{C_F}{N_c} \gamma_0^2 G^{(2)} \\ + \frac{C_F}{N_c} \left[\frac{7}{8} + \frac{C_F}{N_c} \left(\frac{5}{8} - \frac{\pi^2}{6} \right) \right] \gamma_0^2 G_\ell^{(2)}, \end{aligned} \tag{54}$$

which is written in a form similar to (18).

2. Gluon jet

The structure of (49) can be worked out in the same way. The first integral term in its right-hand side is the same as that in (19), such that we can simply set

$$\int_0^1 \mathrm{d}z \frac{\alpha_s}{\pi} \Phi_g^g(z)(G^{(2)}(z) - zG^{(2)}) = \left[\int_0^1 \frac{\mathrm{d}z}{z} \gamma_0^2 G^{(2)}(z)\right] - \frac{11}{12}\gamma_0^2 G^{(2)} + \left(\frac{67}{36} - \frac{\pi^2}{6}\right)\gamma_0^2 G_\ell^{(2)}. \tag{55}$$

The second term provides a contribution

$$\frac{\gamma_0^2}{2N_c} G_{1\ell} G_{2\ell} \int_0^1 \mathrm{d}z \Phi_g^g(z) \ln z \ln(1-z) = \left[\frac{11\pi^2}{36} - \frac{395}{108} + 2\zeta(3)\right]\gamma_0^2 G_{1\ell} G_{2\ell} = \mathcal{O}(\gamma_0^4),$$

that is beyond NMLLA and therefore dropped out here. The second line of (49) simplifies to

$$\begin{aligned}\int_0^1 \mathrm{d}z \frac{\alpha_s}{\pi} n_f \Phi_g^q(z)[2(Q^{(2)}(z) - Q_1(z)Q_2(z)) &- (G^{(2)} - G_1G_2)] \\ &= \frac{n_f T_R}{3N_c}\gamma_0^2[2(Q^{(2)} - Q_1Q_2) - (G^{(2)} - G_1G_2)] \\ &- \frac{13}{18}\frac{n_f T_R}{N_c}\gamma_0^2(Q^{(2)} - Q_1Q_2)_\ell,\end{aligned} \tag{56}$$

and the third one gives

$$\begin{aligned}\int_0^1 \mathrm{d}z \frac{\alpha_s}{\pi} n_f \Phi_g^q(z)(2Q_1(z) - G_1)(2Q_2(1-z) - G_2) &= \frac{n_f T_R}{3N_c}\gamma_0^2(2Q_1 - G_1)(2Q_2 - G_2) \\ &- \frac{13}{18}\frac{n_f T_R}{N_c}\gamma_0^2[(2Q_1 - G_1)Q_{2\ell} \\ &+ (2Q_2 - G_2)Q_{1\ell}].\end{aligned} \tag{57}$$

Gathering (55)–(57) and setting (see Appendix H for further explanations)

$$\begin{aligned} Q &\approx \frac{C_F}{N_c} G + \mathcal{O}(\gamma_0), \\ Q^{(2)} &= \frac{C_F}{N_c} G^{(2)} + \frac{C_F}{N_c}\left(\frac{C_F}{N_c} - 1\right) G_1G_2 + \mathcal{O}(\gamma_0)\end{aligned} \tag{58}$$

in the subleading pieces, we obtain the NMLLA equation for the gluonic correlator

$$(G^{(2)} - G_1G_2)_y = \left[\int_0^1 \frac{\mathrm{d}z}{z}\gamma_0^2 G^{(2)}(z)\right] - \left[\frac{11}{12} + \frac{n_f T_R}{3N_c} \times \left(1 - 2\frac{C_F}{N_c}\right)\right]\gamma_0^2 G^{(2)} + \frac{2n_f T_R}{3N_c} \times \left(1 - \frac{C_F}{N_c}\right)\left(1 - 2\frac{C_F}{N_c}\right)\gamma_0^2 G_1G_2 + \left(\frac{67}{36} - \frac{\pi^2}{6} - \frac{13}{18}\frac{n_f T_R}{N_c}\frac{C_F}{N_c}\right)\gamma_0^2 G_\ell^{(2)} + \left[\frac{13}{9}\frac{n_f T_R}{N_c}\frac{C_F}{N_c}\left(1 - \frac{C_F}{N_c}\right)\right]\gamma_0^2 (G_1G_2)_\ell. \tag{59}$$

The way to get the equations for the correlators $\mathcal{C}_g$ and $\mathcal{C}_q$, to be solved iteratively, proceeds like in Sec. 4 and Appendices A and B of [5].

C. NMLLA correlators

1. Gluon correlator $\mathcal{C}_g$

The differential expression for (21) reads

$$G_{\ell y} = \gamma_0^2 G - a_1\gamma_0^2(\psi_\ell - \beta_0\gamma_0^2)G + a_2\gamma_0^2(\psi_\ell^2 + \psi_{\ell\ell} - \beta_0\gamma_0^2\psi_\ell)G. \tag{60}$$

Differentiating (59) with respect to ℓ gives the following NMLLA differential equation:

$$\begin{aligned}(G^{(2)} - G_1G_2)_{\ell y} = \gamma_0^2 G^{(2)} &- a_1\gamma_0^2(G_\ell^{(2)} - \beta_0\gamma_0^2 G^{(2)}) \\ &+ (a_1 - b_1)\gamma_0^2[(G_1G_2)_\ell - \beta_0\gamma_0^2 G_1G_2] \\ &+ a_2\gamma_0^2(G_{\ell\ell}^{(2)} - \beta_0\gamma_0^2 G_\ell^{(2)}) \\ &+ b_2\gamma_0^2[(G_1G_2)_{\ell\ell} - \beta_0\gamma_0^2(G_1G_2)_\ell],\end{aligned} \tag{61}$$

where a_1, a_2 are given by (24b) and (24b), and with the following coefficients:

$$\begin{aligned} b_1 &= \frac{11}{12} - \frac{n_f T_R}{3N_c}\left(1 - \frac{2C_F}{N_c}\right)^{2\ n_f=3} 0.915, \\ b_2 &= \frac{13}{9}\frac{n_f T_R}{N_c}\frac{C_F}{N_c}\left(1 - \frac{C_F}{N_c}\right)^{n_f=3} 0.18.\end{aligned} \tag{62}$$

Noting $\psi = \ln G$ and $\chi = \ln \mathcal{C}_g$, the second line of (61) can be rewritten in terms of logarithmic derivatives of G and of $\mathcal{C}_g$ (see Appendix I) from which Eq. (61) is solved iteratively. Setting $G^{(2)} = \mathcal{C}_g G_1G_2$ in both members and making use of (60) leads to the analytical solution of (61), valid for arbitrary λ

$$\mathcal{C}_g - 1 = \frac{1 - \delta_1 - b_1(\psi_{1,\ell} + \psi_{2,\ell} - [\beta_0\gamma_0^2]) - [a_1\chi_\ell + \delta_2] + \delta_3}{1 + \Delta + \delta_1 + [a_1(\chi_\ell + [\beta_0\gamma_0^2]) + \delta_2] + \delta_4}, \tag{63}$$

where, like in [5], we introduce $\eta = \ell_2 - \ell_1$. δ_3 and δ_4 are the new NMLLA corrections:

$$\delta_3(\ell_1,\ell_2;\eta) = a_2 f_1(\ell_1,\ell_2;\eta) + b_2 f_2(\ell_1,\ell_2;\eta) = \mathcal{O}(\gamma_0^2),$$
$$\delta_4(\ell_1,\ell_2;\eta) = -a_2 f_3(\ell_1,\ell_2;\eta) = \mathcal{O}(\gamma_0^2), \tag{64}$$

and f_1, f_2 and f_3 are defined in (I1) of appendix A. Setting $\delta_3 = \delta_4 = 0$ in (63), one recovers the exact analytical solution of the corresponding MLLA gluon equation (with $a_2 = b_2 = 0$ in (61)); to derive this formula we have used the same method that was, for the first time, implemented in Appendix A of [5]. The other quantities and their order of magnitude are (see [5])

$$\chi = \ln\mathcal{C}_g, \qquad \chi_\ell = \frac{\mathrm{d}\chi}{\mathrm{d}\ell} = \mathcal{O}(\gamma_0^2), \qquad \chi_y = \frac{\mathrm{d}\chi}{\mathrm{d}y} = \mathcal{O}(\gamma_0^2), \tag{65}$$

$$\psi_i = \ln G_i, \qquad \psi_{i,\ell} = \frac{1}{G_i}\frac{\mathrm{d}G_i}{\mathrm{d}\ell} = \mathcal{O}(\gamma_0), \qquad \psi_{i,y} = \frac{1}{G_i}\frac{\mathrm{d}G_i}{\mathrm{d}y} = \mathcal{O}(\gamma_0), \qquad (i=1,2), \tag{66}$$

$$\Delta = \gamma_0^{-2}(\psi_{1,\ell}\psi_{2,y} + \psi_{1,y}\psi_{2,\ell}) = \mathcal{O}(1), \tag{67}$$

$$\delta_1 = \gamma_0^{-2}[\chi_\ell(\psi_{1,y} + \psi_{2,y}) + \chi_y(\psi_{1,\ell} + \psi_{2,\ell})] = \mathcal{O}(\gamma_0), \tag{68}$$

$$\delta_2 = \gamma_0^{-2}(\chi_\ell\chi_y + \chi_{\ell y}) = \mathcal{O}(\gamma_0^2). \tag{69}$$

To evaluate (65) we consider the bare correlator:

$$\chi = \ln\left[1 + \frac{1 - b_1(\psi_{1,\ell} + \psi_{2,\ell}) + [b_1\beta_0\gamma_0^2]}{1 + \Delta + [a_1\beta_0\gamma_0^2]}\right],$$

the derivatives of which are calculated numerically, to eventually determine (68) and (69).

The analytical result (63) for $\mathcal{C}_g$ will be numerically displayed for the limiting spectrum $\lambda = 0$ in Sec. V D by using (25). For the case $\lambda \neq 0$, we refer the reader to [6] where it has been treated in MLLA by the steepest descent method.

2. Quark correlator $\mathcal{C}_q$

The differential expression of (18) reads

$$Q_{\ell y} = \frac{C_F}{N_c}\left\{\gamma_0^2 G - \frac{3}{4}\gamma_0^2(\psi_\ell - \beta_0\gamma_0^2)G + \tilde{a}_2\gamma_0^2(\psi_\ell^2 + \psi_{\ell\ell} - \beta_0\gamma_0^2\psi_\ell)G\right\}. \tag{70}$$

Differentiating (59) with respect to ℓ gives the NMLLA differential equation

$$(Q^{(2)} - Q_1Q_2)_{\ell y} = \frac{C_F}{N_c}\left\{\gamma_0^2 G^{(2)} - \frac{3}{4}\gamma_0^2(G^{(2)}_\ell - \beta_0\gamma_0^2 G^{(2)}) + \tilde{a}_2\gamma_0^2(G^{(2)}_{\ell\ell} - \beta_0\gamma_0^2 G^{(2)}_\ell)\right\}, \tag{71}$$

to be solved iteratively. Setting $Q^{(2)} = \mathcal{C}_q Q_1 Q_2$ in both members and using (70), one gets the analytical solution (71), valid for arbitrary λ

$$\mathcal{C}_q - 1 = \frac{\frac{N_c}{C_F}\mathcal{C}_g[1 - \frac{3}{4}(\psi_{1,\ell} + \psi_{2,\ell} + [\chi_\ell] - [\beta_0\gamma_0^2]) + \tilde{\delta}_3]\frac{C_F}{N_c}\frac{G_1}{Q_1}\frac{C_F}{N_c}\frac{G_2}{Q_2} - \tilde{\delta}_1 - [\tilde{\delta}_2]}{\tilde{\Delta} + [1 - \frac{3}{4}(\psi_{1,\ell} - [\beta_0\gamma_0^2]) + \tilde{\delta}_{4,1}]\frac{C_F}{N_c}\frac{G_1}{Q_1} + [1 - \frac{3}{4}(\psi_{2,\ell} - [\beta_0\gamma_0^2]) + \tilde{\delta}_{4,2}]\frac{C_F}{N_c}\frac{G_2}{Q_2} + \tilde{\delta}_1 + [\tilde{\delta}_2]}, \tag{72}$$

where $\tilde{\delta}_3$ and $\tilde{\delta}_4$ are the new NMLLA coefficients ($\tilde{a}_2$ is given by (24c))

$$\tilde{\delta}_3(\ell_1,\ell_2;\eta) = \tilde{a}_2 f_1(\ell_1,\ell_2;\eta) = \mathcal{O}(\gamma_0^2),$$
$$\tilde{\delta}_{4,i}(\ell_1,\ell_2;\eta) = \tilde{a}_2 f_4(\ell_1,\ell_2;\eta) = \mathcal{O}(\gamma_0^2). \tag{73}$$

Setting $\tilde{\delta}_3 = \tilde{\delta}_{4,i} = 0$ in (72), one recovers the exact analytical solution of the corresponding MLLA quark equation ($\tilde{a}_2 = 0$ in (71)) that was obtained in the Appendix B of [5]. We have introduced (see [5])

$$\tilde{\Delta} = \gamma_0^{-2}(\varphi_{1,\ell}\varphi_{2,y} + \varphi_{1,y}\varphi_{2,\ell}) = \mathcal{O}(1), \tag{74}$$

$$\tilde{\delta}_1 = \gamma_0^{-2}[\sigma_\ell(\varphi_{1,y} + \varphi_{2,y}) + \sigma_y(\varphi_{1,\ell} + \varphi_{2,\ell})] = \mathcal{O}(\gamma_0), \tag{75}$$

$$\tilde{\delta}_2 = \gamma_0^{-2}(\sigma_\ell\sigma_y + \sigma_{\ell y}) = \mathcal{O}(\gamma_0^2), \tag{76}$$

with $\varphi_k = \ln Q_k$ and $\sigma = \ln\mathcal{C}_q$. For the numerical computation of σ, we take

$$\sigma = \ln\left\{1 + \frac{\frac{N_c}{C_F}\mathcal{C}_g[1 - \frac{3}{4}(\psi_{1,\ell} + \psi_{2,\ell} + [\chi_\ell - \beta_0\gamma_0^2])]\frac{C_F}{N_c}\frac{G_1}{Q_1}\frac{C_F}{N_c}\frac{G_2}{Q_2}}{\tilde{\Delta} + [1 - \frac{3}{4}(\psi_{1,\ell} - [\beta_0\gamma_0^2])]\frac{C_F}{N_c}\frac{G_1}{Q_1} + [1 - \frac{3}{4}(\psi_{2,\ell} - [\beta_0\gamma_0^2])]\frac{C_F}{N_c}\frac{G_2}{Q_2}}\right\}, \tag{77}$$

in which one uses the NMLLA expression (26) for G and Q deduced from (22) and (23), and the exact expression (63) for $\mathcal{C}_g(\ell_1, y_2, \eta)$.

The numerical solution of (72) is given in Sec. V D for $\lambda = 0$. We make the approximation $\varphi_\ell \approx \psi_\ell$, $\varphi_y \approx \psi_y$ that is justified in Appendix E through (E2). We can therefore also use (25). The case $\lambda \neq 0$ was also dealt with at MLLA for a quark jet in [6].

Finally, taking $x_1 = x_2$ in (63) and (72) and going to the asymptotic limit $Q \to \infty$ ($Y \to \infty$), one finds the implicit overall normalization of these observables to be given by those of the multiplicity correlators [32]

$$\mathcal{C}_g \overset{Y\to\infty}{\to} \frac{\langle n_g(n_g-1)\rangle}{\langle n_g\rangle^2} = \frac{4}{3},$$
$$\mathcal{C}_q \overset{Y\to\infty}{\to} \frac{\langle n_q(n_q-1)\rangle}{\langle n_q\rangle^2} = 1 + \frac{N_c}{3C_F},$$

for the gluon and quark jets, respectively. The statement above can be easily explained; the asymptotic expressions of (63) and (72) are, respectively, the DLA formulae (see [8])

$$\mathcal{C}_g(x_1,x_2) \overset{Y\to\infty}{\approx} 1 + \frac{1}{1+\Delta(x_1,x_2)},$$
$$\mathcal{C}_q(x_1,x_2) \overset{Y\to\infty}{\approx} 1 + \frac{N_c}{C_F}\frac{1}{1+\Delta(x_1,x_2)},$$

and $\Delta(x_1, x_2) = 2$ for $x_1 = x_2$ in the same limit.

D. NMLLA corrections versus MLLA

Throughout this analysis, we have consistently incorporated a set of NMLLA corrections. These were not calculated in the previous work [5] which was done at MLLA accuracy for $\lambda = 0$. The philosophy and the basic technique are, however, the same (as well as in [33]). We comment below on the role of these corrections for 2-particle correlations. Both δ_3 and $\tilde{\delta}_3$ are dominated by their leading term, such that

$$\delta_3 \approx (a_2 + b_2)(\psi_{1,\ell} + \psi_{2,\ell})^2 = \mathcal{O}(\gamma_0^2),$$
$$\tilde{\delta}_3 \approx \tilde{a}_2(\psi_{1,\ell} + \psi_{2,\ell})^2 = \mathcal{O}(\gamma_0^2).$$

Since both $a_2 + b_2$ and $\tilde{a}_2$ are positive and ψ_ℓ increases as $\ell \to 0$, NMLLA corrections are expected to increase the MLLA solution of [5] in the limit $\ell_1 + \ell_2 \to 0$, as can be seen in (63) and (72). Thus, as found for the single-inclusive $k_\perp$-distribution, the (x_1, x_2) domain in which the two particles are "correlated," i.e. $\mathcal{C}_{g,q} - 1 > 0$, becomes larger than at MLLA. In the limit $\ell_1 + \ell_2 \to 2Y$, the role of the new corrections is, on the contrary, expected to vanish since $\psi_\ell \to 0$ when $\ell \to Y$.

This is indeed what appears in Figs. 12 and 13, which compare the MLLA and NMLLA solutions at the Tevatron energy scale ($Q = 155$ GeV). While Eqs. (63) and (72) are general analytical solutions of the evolution equations at $\lambda \neq 0$, the numerical results displayed below are calculated at the limiting spectrum $\lambda = 0$, by plugging the formula (25) for the inclusive spectrum into (63) and (72).

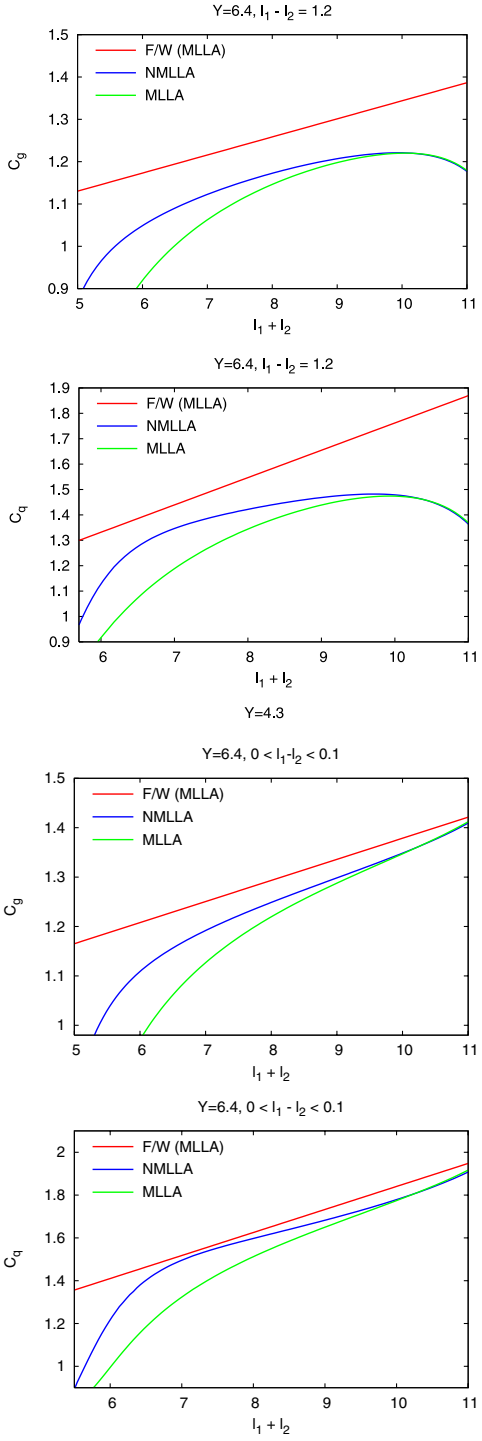

FIG. 12 (color online). 2-particle correlations as a function of $\ell_1 + \ell_2$ for $\ell_1 - \ell_2 = 1.2$ (top) and $\ell_1 \approx \ell_2$ (bottom), successively for a gluon jet and a quark jet: on each figure are displayed MLLA (bottom), NMLLA (middle) and Fong-Webber (top) [34] predictions.

The four lines in Fig. 14 show the positions in (ℓ_1, ℓ_2) space corresponding to the curves of Figs. 12 and 13. The two upper curves of Fig. 12 correspond to line 2, its two lower curves to line 1; the two upper curves of Fig. 13 correspond to line 3, and its two lower curves to line 4.

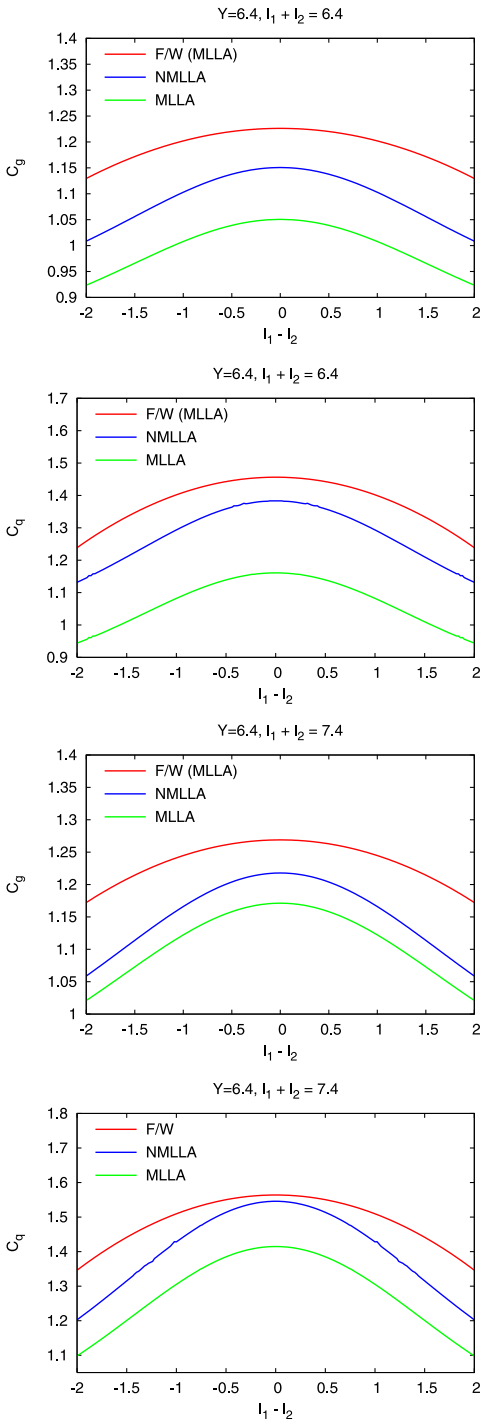

FIG. 13 (color online). 2-particle correlations as a function of $\ell_1 - \ell_2$ for $\ell_1 + \ell_2 = 6.4$ (top) and $\ell_1 + \ell_2 = 7.4$ (bottom), successively for a gluon jet and a quark jet: on each figure are displayed MLLA (bottom), NMLLA (middle) and Fong-Webber (top) [34] predictions.

The correlations displayed in Figs. 12 and 13 appear more important in NMLLA than in MLLA. Physically, because the recoil of each emitting parton is better taken into account in the former approximation, less energy

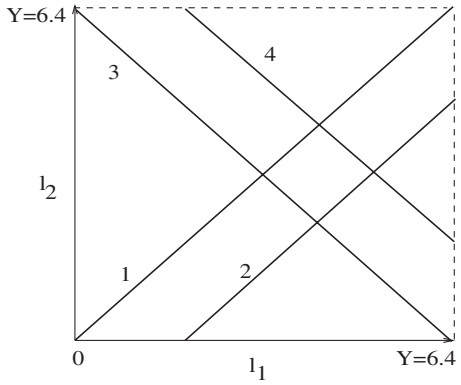

FIG. 14. Positions in (ℓ_1, ℓ_2) space of Figs. 12 and 13.

becomes available and the multiplicity of emitted particles is expected to decrease. Consequently, inside a bunch of a fewer number of particles, two among them get more correlated.

E. Dependence on $\Lambda_{\rm QCD}$

We have tested the dependence of the gluonic correlation function $\mathcal{C}_g$ on $\Lambda_{\rm QCD}$, by varying it from 150 MeV to 500 MeV. The results are displayed in Fig. 15, as a function of $\ell_1 + \ell_2$ (top) and $\ell_1 - \ell_2$ (bottom). Variations are seen to stay below 10%.

F. Comparison with Fong and Webber MLLA predictions

The comparison with the predictions by Fong and Webber [34] is also instructive. Let us recall that their calculation is done at MLLA, yet obtained from the exact result of [5] when the two outgoing partons are taken to be close to the peak of the inclusive spectrum, and when the exact solution is expanded at first order in $\sqrt{\alpha_s}$. From the present results and that of [5], we can conclude that:

(i) the convergence of the series obtained by expanding the exact MLLA result in powers of $\sqrt{\alpha_s}$ is very bad; if one proceeds in this way, NMLLA corrections may be as large as MLLA, making the series meaningless; note that similar conclusions have been obtained in [9] when dealing with recoil effects and, more precisely, with the role of exact kinematics in the bounds of integrations;

(ii) instead, in the procedure that has been adopted here, i.e. finding exact NMLLA solutions of the (approximate) MLLA evolution equations, NMLLA corrections turn out to be under control and their inclusion brings the predictions closer to Fong and Webber's.

The present study, together with [5], consequently stresses the importance of dealing with *exact* solutions of the evolution equations in jet calculus.

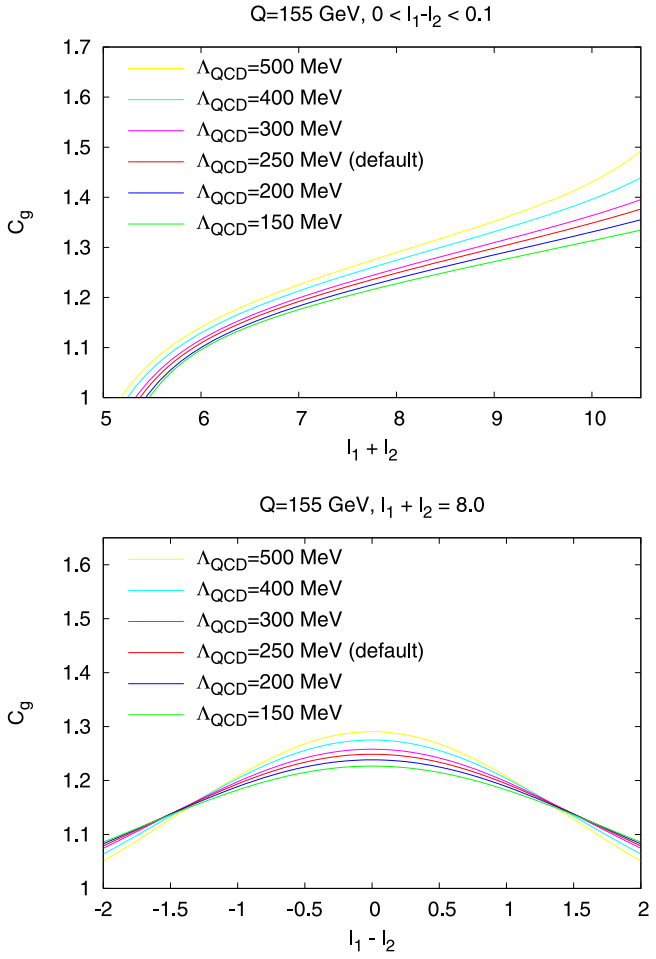

FIG. 15 (color online). Dependence of the gluonic 2-particle correlation function C_g on $\Lambda_{\rm QCD}$. The curves and the values of $\Lambda_{\rm QCD}$ indicated in the caption are set in the same order.

VI. DISCUSSION AND SUMMARY

A. Discussion

Energy conservation is a fundamental issue in jet calculus. While it is well known that the complete neglect of the recoil of the emitting parton leads to DLA (taking only into account the singular parts of the splitting functions), the MLLA, in which "single logarithms" are added to DLA, takes partial account of the recoil. Corrections appearing at higher orders in an expansion in powers of $\sqrt{\alpha_s}$ come from (i) the shifts by $\ln z$ and $\ln(1-z)$ in the arguments of the hadronic fragmentation functions; (ii) the nonsingular terms in the splitting functions; and (iii) the running of α_s. Our line of approach in this paper was accordingly the following:

(i) we considered MLLA evolution equations as kinetic equations of QCD, and expanded their (exact) analytical solutions in powers of $\sqrt{\alpha_s}$ up to the order $\mathcal{O}(\alpha_s)$. Contributions that do not fit into such an framework are discarded;

(ii) we stuck to the logic advocated in [14,33,35] that, at small x and for $|\ln z| \sim |\ln(1-z)| \ll \ln(1/x)$, the successive corrections, MLLA, NMLLA, etc., which better and better account for energy conservation, are taken care of by a systematic expansion in powers of $\ln z$ and $\ln(1-z)$.

The size of the NMLLA terms depends on the precise definition of $\Lambda_{\rm QCD}$: a rescaling of $\Lambda_{\rm QCD}$ would change the terms at this order. Systematically solving this problem would require a 2-loop calculation which has not been obtained so far for any multiplicity-related observable. We therefore have to consider here $\Lambda_{\rm QCD}$ as a phenomenological parameter. The sensitivity of our results to variations of $\Lambda_{\rm QCD}$ have been studied and found moderate (20% for inclusive $k_\perp$-distribution and less than 10% for correlations) when $\Lambda_{\rm QCD} \to 2\Lambda_{\rm QCD}$.

We left aside the question of the matching of the two definitions of the jet axis, "inclusive" direction of the energy flow in this work, and "exclusive" fixing from all outgoing hadrons in experiments.

Last, hints that the NMLLA correction that has been considered here is the dominant one can already be found in [10], where this type of NMLLA recoil effect was shown to drastically affect particle multiplicities and particle correlations through a factor proportional to the number of partons involved in the process. This however only concerns *a priori* 2-particle correlations. Spanning a gate between the Koba-Nielsen-Olesen [36]phenomenon and the techniques that we have used here stays a challenging task which we hope to achieve in the future.

Since calculated NMLLA corrections proved to be quite substantial, a natural question arises concerning the magnitude of higher-order corrections. There, in correlation with the remarks at the end of the introduction of Sec. II, it seems legitimate to consider that, since this observable is mainly sensitive to soft particles, the corrections are expected to be moderate. This can be different for integrated quantities like multiplicities.

B. Summary

In this work, we have computed next-to-MLLA corrections to the single-inclusive $k_\perp$-distributions as well as 2-particle momentum correlations inside a jet at high-energy colliders. It comes as a natural extension of [4,5] in which MLLA results are provided. In particular, it exploits the same logic of using, at small energy-fraction x of the emitted hadron, exact solutions to (approximate) evolution equations for the inclusive spectrum. The technique used is based on a systematic expansion in powers of $\sqrt{\alpha_s}$ which neglects nonperturbative effects. Nevertheless, it proves to be remarkably efficient to describe the preliminary measurements of (the shape of) the $k_\perp$-differential inclusive cross section performed by CDF [7]. This is an indication that nonperturbative contributions play a small role in this

observable, and concentrates in the overall normalization. (LPHD hypothesis is tantamount to stating that in this universal factor lies the trace of the [soft and local] hadronization process.) The transition from MLLA to next-to-MLLA enlarges considerably the domain where the computations agree with the experimental data, both in the transverse momentum of hadrons and in their energy-fraction x.

In our analysis, single-inclusive x-distributions as well as $k_\perp$-spectra have been determined exactly beyond the limiting spectrum approximation, i.e. for arbitrary $Q_0 \neq \Lambda_{\rm QCD}$. This should, in particular, be relevant when dealing with distributions of rather massive hadrons [24]. In this respect, experimental identification of outgoing hadrons could provide precious additional tests of LPHD and of the physical interpretation of the infrared cutoff Q_0 as the "hadronization scale." As far as 2-particle correlations inside a jet are concerned, future results from LHC, in addition to the ones of OPAL [37] and recent ones from CDF [38], are waited for to be compared with the NMLLA predictions presented in this study.

The limitations of the method are in particular:

(i) neglecting nonperturbative contributions may prove less justified for not so inclusive observables. In that respect, forthcoming data on 2-particle correlations from LHC promise to be very instructive. While incorporating some nonperturbative contributions is not excluded *a priori*, a systematic way to handle them is of course still out of reach;

(ii) the absolute normalization of the distributions, which involve nonperturbative effects (hadronization) is not predicted;

(iii) the calculation is performed in the small-x limit and extrapolation to larger x may become problematic. The transition to larger x, or from MLLA to DGLAP evolution equations, is undoubtedly also a very important issue. It may be tempting to proceed in this direction by going to higher orders in the expansion initiated in [4–6] and extended in the present work. However, the universality of MLLA evolution equations as kinetic equations of QCD should be cast on firmer grounds.

C. Perspective: going to larger x

A Taylor expansion, when used inside evolution equations, was already advocated long ago to better account for energy conservation [33,35]. It appears fairly easy to realize that pushing it at higher and higher orders of $\ln u$ at small x inside the convolution integral (29) should play a role in it extending the domain of reliability of the solution to larger and larger values of x. Indeed, in (29), one integrates from $u = x$ to $u = 1$ a certain function $F(\ln u - \ln x)$. F is expanded at large $|\ln x|$ around $|\ln u| = 0$, which corresponds to $u = 1$. If one increases x, the domain of integration shrinks closer and closer to its upper bound $u = 1$. Suppose that we set $x = 1 - \epsilon$. The integral becomes $\int_{1-\epsilon}^{1} du F(\ln u - \ln(1-\epsilon))$. Now, in the argument of F, for all u in the domain of integration $|\ln u| \sim |\ln x|$, such that a reliable expansion of F, if it exists (it depends on its radius of convergence), must involve a large number of terms. This is like expanding a function $f(t-a)$ around $f(-a)$: for $|a| \sim |\ln x| \gg t \sim \ln u \approx \ln 1$, a few powers of t provide a good approximation to $f(t-a)$, but when a decreases, expanding $f(t-a)$ around $f(-a)$ uses an expansion parameter t of the same order of magnitude as a itself. We conclude that *increasing* x requires going to higher and higher orders in the expansion of F in powers of $|\ln u|$. Conversely, going to higher and higher order in this expansion is expected to yield a solution valid in a larger and larger domain of x.

When applied to the evolution equations themselves, and to the similar expansion in powers of $(\ln z)$ that we did in Sec. II, the same kind of arguments apply, which are not unrelated with the link between MLLA and DGLAP evolution equations. Since NMLLA corrections to 2-particle correlations, unlike the ones for the inclusive $k_\perp$ distribution, are directly connected with NMLLA corrections to the evolution equations themselves, it is worth a few comments concerning this issue.

(a) That MLLA evolution Eqs. (4) and (5) are, at least for inclusive enough observables, valid in a much broader x domain than has been known for a long time [8]. It was furthermore noticed some years ago [15] that, for parton multiplicities, the exact numerical solution of MLLA evolution equations perfectly matched experimental results in a very large domain, and that, accordingly, the MLLA evolution equations contain more information than expected and the problems of finding their analytical solutions are essentially of technical nature;

(b) at small x MLLA evolution equations are identical to DGLAP evolution equations but for a shift by $\ln z$ (z is the integration variable) of the variable $Y = y + \ell$ which controls the evolution of the jet hardness [5,8];

(c) for soft outgoing hadrons (x small $\Leftrightarrow |\ell| \equiv |\ln x|$ large), this shift is negligible in the hard parton region ($|\ln z| < |\ln x|$). However, when going to harder hadrons, that is when x grows, $|\ell|$ decreases and $|\ln z|$ is no longer negligible. When it is so, the function to integrate is no longer safely approximated by its 0th order expansion (corresponding to $\ln z = 0$) and higher powers of $\ln z$ are needed. This provides, in addition to the argumentation at the beginning of this subsection, another link between this expansion at higher orders and going to larger x;

(d) accordingly, the Taylor expansion that we used inside MLLA evolution equations, which extends their "validity" to larger x, may contribute to span-

ning a bridge between them and DGLAP evolution equations (see for example [39,40]).

ACKNOWLEDGMENTS

It is pleasure to thank Yu. L. Dokshitzer, I. M. Dremin and W. Ochs for illuminating discussions. We also thank S. Jindariani (CDF) for an invaluable exchange of information concerning CDF data.

APPENDIX A: NMLLA CORRECTIONS NEGLECTED IN THE DERIVATION OF THE APPROXIMATE EQUATIONS FOR THE INCLUSIVE SPECTRUM

To get a self-contained equation for the inclusive spectrum inside a gluon jet, one needs to plug in consistently

$$\begin{aligned} Q &= \frac{C_F}{N_c}[1 + (a_1 - \tilde{a}_1)\psi_\ell]G + \mathcal{O}(\gamma_0^2), \\ Q_\ell &= \frac{C_F}{N_c}G_\ell + \mathcal{O}(\gamma_0^2) \end{aligned} \tag{A1}$$

respectively, in the first and second terms of the right-hand side of (20). Taking into account the correction proportional to ψ_ℓ in (A1) would provide an extra term

$$\ldots + \frac{2}{3}\frac{n_f T_R}{N_c}\frac{C_F}{N_c}(a_1 - \tilde{a}_1)G_\ell$$

which adds to the right-hand side of (21) and slightly changes the value of a_2 (24d) from 0.06 to 0.08; this number is also small, such that the approximation that we justify in Appendix B remains valid.

APPENDIX B: STEEPEST DESCENT EVALUATION OF (23) FOR CONSTANT γ_0^2

We solve the self-contained gluon Eq. (23) with frozen α_s by performing the Mellin's transform

$$G(\ell, y) = \iint_C \frac{d\omega d\nu}{(2\pi i)^2} e^{\omega\ell} e^{\nu y} \mathcal{G}(\omega, \nu). \tag{B1}$$

The contour of integration (C) lies to the right of all poles, and $\mathcal{G}(\omega, \nu)$ is the "propagator" in Mellin's space. Plugging (B1) into (23) yields

$$G(\ell, y) = \int_C \frac{d\omega}{2\pi i} \exp\left[\omega\ell + \gamma_0^2\left(\frac{1}{\omega} - a_1\right)y + a_2\gamma_0^2\omega y\right]. \tag{B2}$$

The simplest way to estimate the previous Mellin's representation is by substituting the DLA saddle point $\omega_0 = \gamma_0\sqrt{\frac{y}{\ell}}$ into the MLLA ($\propto a_1$) and NMLLA ($\propto a_2$) terms. Doing so, the steepest descent evaluation of the inclusive spectrum at fixed α_s in the limit $\ell \gg 1$ ($x \ll 1$) leads to

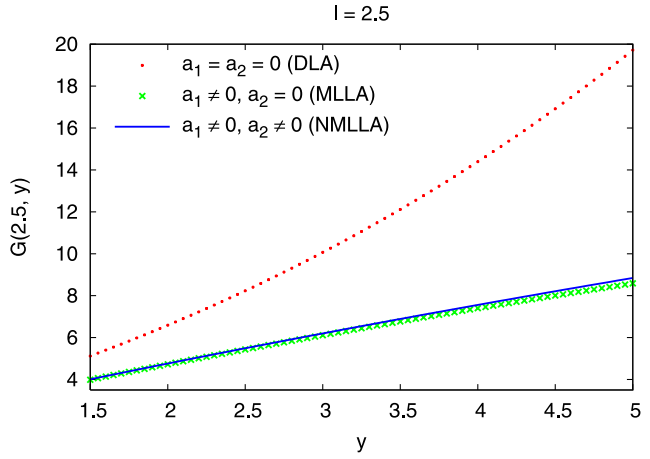

FIG. 16 (color online). Single-inclusive spectrum at fixed α_s as a function of y at $Y_{\Theta_0} = 7.5$ and $\ell = 2.5$.

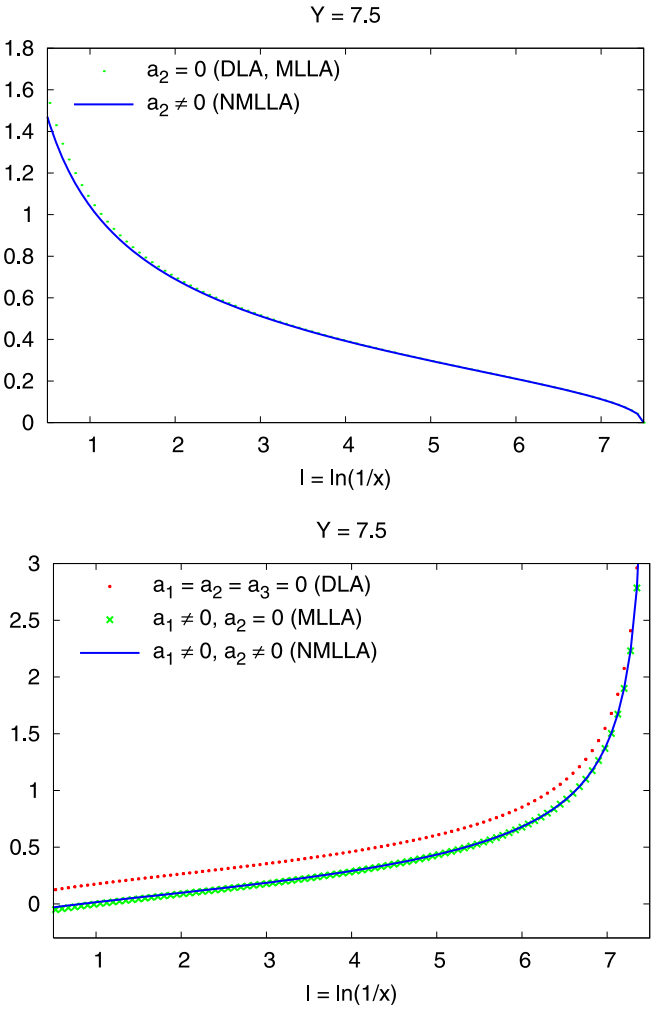

FIG. 17 (color online). Logarithmic derivatives ψ_ℓ (top) and ψ_y (bottom) of the inclusive spectrum $G(\ell, Y_{\Theta_0})$ at $Y_{\Theta_0} = 7.5$.

$$G(\ell, y) \approx \frac{1}{2}\sqrt{\frac{\gamma_0 y^{1/2}}{\pi \ell}} \exp\left(2\gamma_0\sqrt{\ell y} - a_1\gamma_0^2 y + a_2\gamma_0^3 y\sqrt{\frac{y}{\ell}}\right). \tag{B3}$$

The result, plotted on Fig. 16 together with the DLA and MLLA results (still at fixed α_s), shows no significant difference between the MLLA and NMLLA solutions.

We can therefore safely use the exact MLLA solution (25) to compute the NMLLA inclusive $k_\perp$-distribution. Likewise, the logarithmic derivatives $\psi_\ell = G_\ell/G$ and $\psi_y = G_y/G$

$$\begin{aligned}\psi_\ell(\ell, y) &= \gamma_0\sqrt{\frac{y}{\ell}} - \frac{1}{2}a_2\gamma_0^3\left(\frac{y}{\ell}\right)^{3/2},\\ \psi_y(\ell, y) &= \gamma_0\sqrt{\frac{\ell}{y}} - a_1\gamma_0^2 + \frac{3}{2}a_2\gamma_0^3\sqrt{\frac{y}{\ell}},\end{aligned} \tag{B4}$$

which are used to evaluate 2-particle correlation, are displayed in Fig. 17 as a function of $\ell = Y_\Theta - y$.

There, again, the difference between MLLA and NMLLA is negligible, such that the exact MLLA expression of the single-inclusive distribution can be taken as a good approximation in the evaluation of NMLLA 2-particle correlations.

APPENDIX C: SECOND DERIVATIVE OF THE SPECTRUM $G_{\ell\ell}$ AT $\lambda = 0$

The expression of the second derivative of the inclusive spectrum for a gluon jet reads

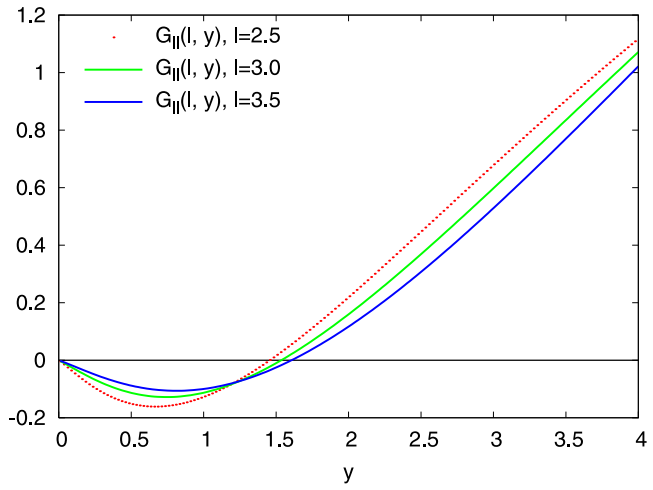

FIG. 18 (color online). Second derivative of the single-inclusive spectrum as a function of y at $Y_{\Theta_0} = 7.5$.

$$\begin{aligned}G_{\ell\ell}(\ell, y) &\equiv G(\ell, y)(\psi_{g,\ell}^2 + \psi_{g,\ell\ell})(\ell, y)\\ &= \frac{2}{\ell + y}\left(G_\ell(\ell, y) - \frac{1}{\ell + y}G(\ell, y)\right) + \frac{\Gamma(B)}{\beta_0}\\ &\times \int_{-(\pi/2)}^{\pi/2}\frac{d\alpha}{\pi}e^{-(B-2)\alpha}\left[\frac{1}{\beta_0^2}\mathcal{F}_{B+2} + \frac{6}{\beta_0(\ell + y)}\right.\\ &\left.\times \sinh\alpha\,\mathcal{F}_{B+1} + \frac{8}{(\ell + y)^2}\sinh^2\alpha\,\mathcal{F}_B\right].\end{aligned} \tag{C1}$$

I_B is the modified Bessel function of the first kind. $G_{\ell\ell}$ is displayed in Fig. 18 as a function of y for three values of ℓ. We notice that it is negative at small values of y and gets positive at larger y.

APPENDIX D: SCALING VIOLATIONS

Varying $uE\Theta$ to $E\Theta$ in the argument of the DGLAP splitting function $D^A_{A_0}$ in (37) yields corrections of relative magnitude $\mathcal{O}(\alpha_s)$ which are accordingly NMLLA. We need to estimate

$$\int_x^1 duuD^A_{A_0}(u, E\Theta_0, uE\Theta) \equiv \int_x^1 duuD^A_{A_0}(u, \xi(u)) \tag{D1}$$

where

$$\xi(u) = \frac{1}{b}\ln\left(\frac{\ln\frac{E\Theta_0}{\Lambda}}{\ln\frac{uE\Theta}{\Lambda}}\right); \qquad b = 4N_c\beta_0.$$

Writing

$$D^A_{A_0}(u, E\Theta_0, uE\Theta) = e^{\ln u(d/(d\ln(E\Theta)))}D^A_{A_0}(u, E\Theta_0, E\Theta),$$

where

$$\frac{d}{d\ln(E\Theta)} = \frac{d}{d\xi}\frac{d\xi}{d\ln(E\Theta)} = -\frac{1}{b}\frac{1}{\ln(E\Theta)}\frac{d}{d\xi},$$

leads to

$$e^{\ln u(d/(d\ln(E\Theta)))} = 1 - \frac{1}{b}\frac{\ln u}{\ln(E\Theta)}\frac{d}{d\xi} + \mathcal{O}(\alpha_s^2).$$

Finally, (D1) can be approximated by

$$\begin{aligned}\int_x^1 duuD^A_{A_0}(u, E\Theta_0, uE\Theta) &\approx \int_x^1 duuD^A_{A_0}(u, E\Theta_0, E\Theta)\\ &- \frac{1}{b}\frac{1}{\ln\frac{E\Theta}{\Lambda}}\int_x^1 duu\ln u\frac{\partial D^A_{A_0}}{\partial\xi}\\ &\times(u, \xi(u = 1)) + \mathcal{O}(\alpha_s^2).\end{aligned}$$

We can now estimate the order of magnitude of this correction, taking, for example, the analytic form of $D^q_q(u)$ (nonsinglet combination of quark distributions) in the $u \to 1$ limit [8,41]

$$D^q_q(u) \sim (1 - u)^{-1+4C_F\xi}$$

with $\xi = \xi(u = 1) = \frac{1}{b}\ln(\frac{Y_{\Theta_0}}{Y_\Theta})$. We need to compare

$$I = \int_x^1 duu(1-u)^{-1+4C_F\xi}$$

with

$$\delta I = \frac{4C_F}{b(\ell+y+\lambda)} \int_x^1 duu \ln u \ln(1-u)(1-u)^{-1+4C_F\xi(u=1)}.$$

Taking, for instance, $\xi(Y_{\Theta_0}=6, Y_\Theta=3)=0.08$, which is a typical value at LEP or Tevatron energy scales, one finds $\delta I/I \approx 0.04$. When $Y_\Theta \to Y_{\Theta_0}$, this ratio tends very fast to 0, such that the role of this correction at larger $k_\perp$ is negligible.

APPENDIX E: EXACT VERSUS APPROXIMATE NMLLA COLOR CURRENTS

Using (26) yields the following exact (in the sense that it takes into account all subleading corrections coming from (26)) expression for the color currents

$$\begin{aligned}\langle C\rangle_i^{\text{exact}}(\ell,y) = \langle C\rangle_i^{\text{approx}}(\ell,y) + \langle u\rangle_i^q(\ell,y)\frac{C_F}{N_c}[(a_1-\tilde{a}_1) \\ \times \psi_{g,\ell}(\ell,y) + (a_1(a_1-\tilde{a}_1)+\tilde{a}_2-a_2) \\ \times (\psi_{g,\ell}^2+\psi_{g,\ell\ell})(\ell,y)] + \delta\langle u\rangle_i^q(\ell,y) \\ \times \frac{C_F}{N_c}(a_1-\tilde{a}_1)\psi_{g,\ell}^2(\ell,y) + \mathcal{O}(\gamma_0^2), \quad \text{(E1)}\end{aligned}$$

where $i = g, q$, and $\langle u\rangle_i^q$ are given in [5]. The approximate expression, used in the core of the paper, only keeps $(C_F/N_c)G$ in (26).

In Fig. 19, the exact and approximate color currents are shown to be in practice indistinguishable, which justifies the use of the latter in the core of the paper.

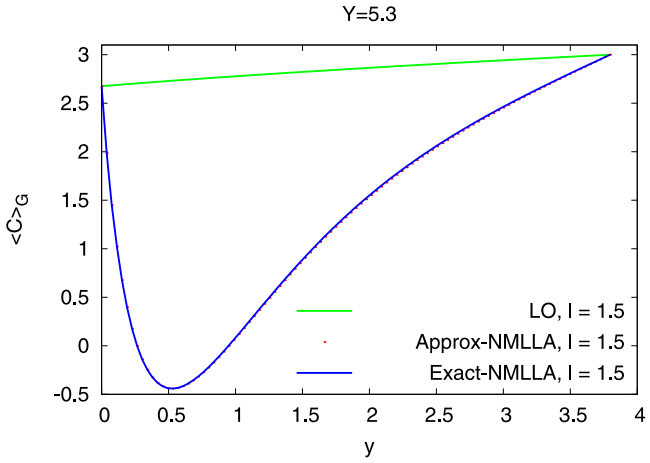

FIG. 19 (color online). Approximate (used in the core of the paper) and exact color currents for a gluon jet.

We also performed the following approximation to evaluate the color current:

$$\begin{aligned}\varphi_\ell \equiv \psi_{q,\ell} &= \psi_{g,\ell}\left[1+(a_1-\tilde{a}_1)\left(\frac{G_{\ell\ell}}{G_\ell}-\frac{G_\ell}{G}\right)\right]+\mathcal{O}(\gamma_0^2) \\ &\approx \psi_{g,\ell} \equiv \psi_\ell. \quad \text{(E2)}\end{aligned}$$

In fact, $(a_1-\tilde{a}_1)\approx 0.18$ and $G_{\ell\ell}/G_\ell \sim G_\ell/G = \mathcal{O}(\gamma_0)$. These approximations were also made and numerically tested in [4,5] (see, for example, Fig. 20 in [5]).

APPENDIX F: EXPRESSION OF $\delta\langle C\rangle_{\tilde{A}_0}^{\text{NMLLA}-\text{MLLA}}$

A straightforward calculation that follows from (41) gives, respectively, for the gluon and quark jets, the following results:

$$\begin{aligned}\delta\langle C\rangle_g^{\text{NMLLA}-\text{MLLA}} = \frac{1}{2}\Bigg[12.7394\left(-1.49751-\frac{1}{9}\ln\frac{\ell+y+\lambda}{Y_{\Theta_0}+\lambda}\right)\left(-0.260721-\frac{1}{9}\ln\frac{\ell+y+\lambda}{Y_{\Theta_0}+\lambda}\right)\left(\frac{\ell+y+\lambda}{Y_{\Theta_0}+\lambda}\right)^{50/81} \\ + 356.711\left(-0.0369486-\frac{1}{9}\ln\frac{\ell+y+\lambda}{Y_{\Theta_0}+\lambda}\right)\left(0.377382-\frac{1}{9}\ln\frac{\ell+y+\lambda}{Y_{\Theta_0}+\lambda}\right)\Bigg](\psi_{g,\ell}^2+\psi_{g,\ell\ell}), \\ \delta\langle C\rangle_q^{\text{NMLLA}-\text{MLLA}} = \frac{1}{2}\Bigg[-22.6479\left(-0.936071-\frac{1}{9}\ln\frac{\ell+y+\lambda}{Y_{\Theta_0}+\lambda}\right)\left(0.164816-\frac{1}{9}\ln\frac{\ell+y+\lambda}{Y_{\Theta_0}+\lambda}\right)\left(\frac{\ell+y+\lambda}{Y_{\Theta_0}+\lambda}\right)^{50/81} \\ + 356.711\left(-0.0635496-\frac{1}{9}\ln\frac{\ell+y+\lambda}{Y_{\Theta_0}+\lambda}\right)\left(0.154028-\frac{1}{9}\ln\frac{\ell+y+\lambda}{Y_{\Theta_0}+\lambda}\right)\Bigg](\psi_{g,\ell}^2+\psi_{g,\ell\ell}),\end{aligned}$$

where the expression and behavior of the function $(\psi_{g,\ell}^2+\psi_{g,\ell\ell})$ are given in Appendix C.

APPENDIX G: FIXING AND VARYING ℓ_{min}

Our small x calculation cannot be trusted below a certain ℓ_{min}, otherwise, as shown in Fig. 20, $\mathrm{d}^2N/\mathrm{d}\ell\mathrm{d}y$ gets negative in the perturbative domain.

We give in Table I values of ℓ_{min} as they come out from the requirement of positivity, for different values of the jet hardness (and the corresponding maximal values of y).

ℓ_{min} is not an intrinsic (physical) characteristic of the system under concern (gluon or quark jet), it is only an *ad hoc* parameter below which poor credibility can be attached to the results. One notices in Table I that, at a given Q, the ℓ_{min} for a quark jet is always larger than the one for a gluon jet; this only means that our calculations can be pushed to larger x for gluons than for quarks without encountering problems of positivity. The question then arises whether, in calculating the inclusive $k_\perp$ distribution of a mixed jet, one should attach the same ℓ_{min} to each of its

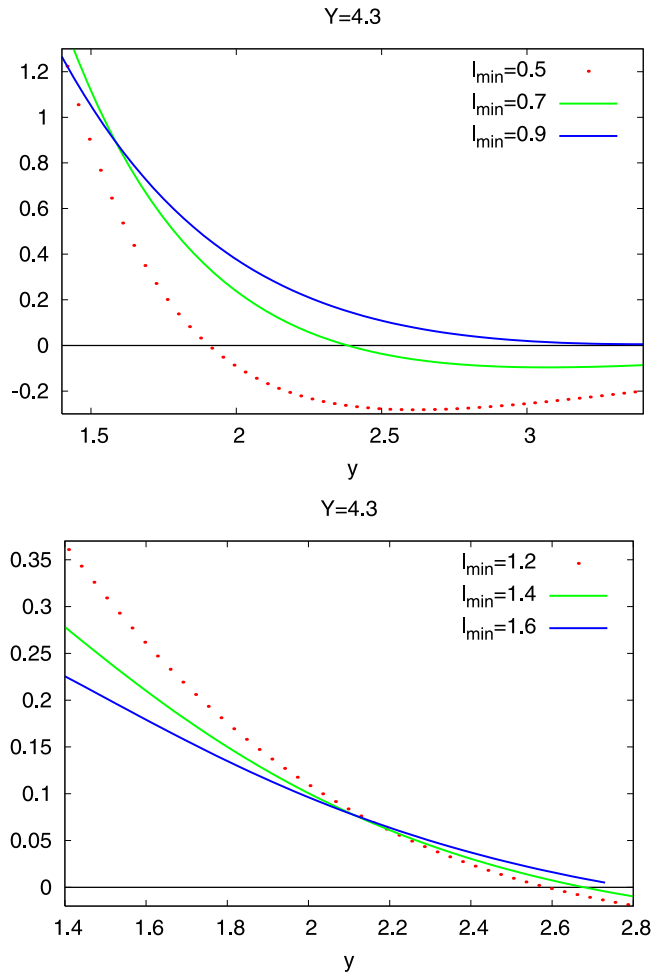

FIG. 20 (color online). $\frac{d^2N}{d\ell dy}$ for a gluon jet (top) and a quark jet (bottom) as a function of y for three values of ℓ.

components, which can only be, of course, the larger one, that is, the one of the quark component, or give to each component its proper value of $\ell_{\min}$ as given in Table I. The simple answer to this question comes from the fact that the two choices give, in practice, extremely close results. Deeper considerations on which $\ell_{\min}$ should be chosen are thus irrelevant.

TABLE I. Values of $\ell_{\min}$ and $y_{\max}$ for different values of the jet hardness.

Q (GeV)	Y_{Θ_0}	$\ell^g_{\min}$	$y^g_{\max}$	$\ell^q_{\min}$	$y^q_{\max}$
19 (CDF)	4.3	0.9	3.4	1.6	2.7
27 (CDF)	4.7	1.0	3.8	1.7	3.1
37 (CDF)	5.0	1.0	4.1	1.8	3.4
50 (CDF)	5.3	1.1	4.4	1.9	3.7
68 (CDF)	5.6	1.1	4.7	2.0	4.0
90 (CDF)	5.9	1.2	5.0	2.0	4.3
119 (CDF)	6.2	1.2	5.3	2.1	4.6
155 (CDF)	6.4	1.3	5.4	2.2	4.7
450 (LHC)	7.5	1.4	6.1	2.4	5.1

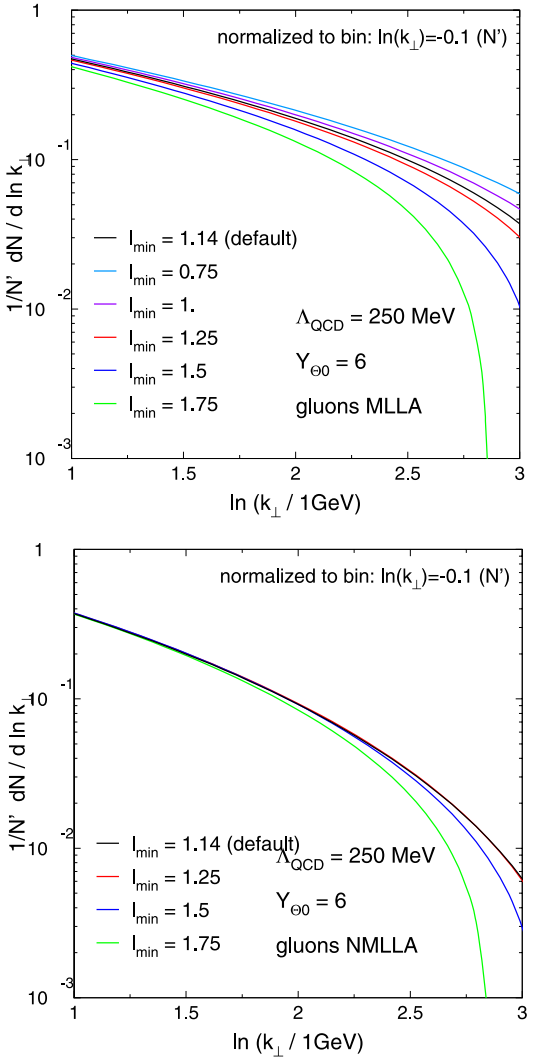

FIG. 21 (color online). The dependence on $\ell^g_{\min}$ of the inclusive gluon $k_\perp$ distribution for $Y_{\Theta_0} = 6$ at MLLA (top) and NMLLA (bottom). The curves and the values of $\ell_{\min}$ indicated in the caption are set in the same order.

For the sake of completeness, we plot in Fig. 21 the inclusive gluon $k_\perp$-distribution at $Y_{\Theta_0} = 6$, for different values of $\ell^g_{\min}$, both at MLLA (top) and NMLLA (bottom). Changing $\ell^g_{\min}$ from 1 to 1.5 modifies the NMLLA spectrum by no more than 20% for $\log(k_\perp/1\ \text{GeV}) = 2.5$. At MLLA, the dependence proves much more dramatic.

Like for the variation with Λ_{QCD} in Sec. III E, that the variations with $\ell_{\min}$ seem to increase with $k_\perp$ is only an artifact due to the normalization at the first bin.

APPENDIX H: NMLLA TERMS NEGLECTED IN V B

The approximations we have made in (58) needs further comments; indeed one has to replace Q and $Q^{(2)}$ by the full MLLA expressions

$$Q = \frac{C_F}{N_c}[1 + (a_1 - \tilde{a}_1)\psi_\ell]G + \mathcal{O}(\gamma_0^2), \tag{H1}$$

$$\frac{\frac{Q^{(2)}}{Q_1 Q_2} - 1}{\frac{G^{(2)}}{G_1 G_2} - 1} = \frac{N_c}{C_F}\left[1 + (b_1 - a_1)(\psi_{\ell_1} + \psi_{\ell_2})\frac{1+\Delta}{2+\Delta}\right] + \mathcal{O}(\gamma_0^2) \tag{H2}$$

respectively. b_1 is defined in (62) and

$$\Delta = \gamma_0^{-2}(\psi_{1,\ell}\psi_{2,y} + \psi_{1,y}\psi_{2,\ell}) = \mathcal{O}(1), \qquad \psi_\ell = \mathcal{O}(\gamma_0).$$

(H2) was obtained in [5] and displayed later in [6]. Working out the structure of (H2) after we have inserted (H1), leads to

$$\begin{aligned} Q^{(2)} = {} & \frac{C_F}{N_c}G^{(2)} + \frac{C_F}{N_c}\left(\frac{C_F}{N_c} - 1\right)G_1G_2 + \frac{C_F}{N_c}(b_1 - a_1) \\ & \times (\psi_{\ell_1} + \psi_{\ell_2})\frac{1+\Delta}{2+\Delta}(G^{(2)} - G_1G_2) + \frac{C_F}{N_c}(a_1 - \tilde{a}_1) \\ & \times (\psi_{\ell,1} + \psi_{\ell,2})(G^{(2)} - G_1G_2) + \frac{C_F^2}{N_c^2}(a_1 - \tilde{a}_1) \\ & \times (\psi_{\ell_1} + \psi_{\ell_2})G_1G_2 + \mathcal{O}(\gamma_0^2). \end{aligned} \tag{H3}$$

As already mentioned in [6], the coefficient $(b_1 - a_1)$, which is color suppressed, is $\simeq 10^{-2}$, $\psi_\ell \simeq 10^{-1}$ and $\frac{1+\Delta}{2+\Delta} \simeq \frac{3}{4}$. Thus, the whole correction is roughly $\simeq 10^{-4}$. This is why it is not taken into account here, which allows for analytic results. Introducing the terms of (H3) $\propto (a_1 - \tilde{a}_1)$ in the right-hand side of (56) provides extra terms

$$\begin{aligned} & \ldots + \frac{2n_f T_R}{3N_c}\frac{C_F}{N_c}(a_1 - \tilde{a}_1)(\psi_{\ell,1} + \psi_{\ell,2})\gamma_0^2(G^{(2)} - G_1G_2) \\ & + \frac{2n_f T_R}{3N_c}\frac{C_F^2}{N_c^2}(a_1 - \tilde{a}_1)\gamma_0^2(G_1G_2)_\ell \end{aligned}$$

which add to the right-hand side of (59). They are both, in particular, color suppressed, the first one by a factor $\propto 1/N_c^2$ and the second one by $\propto 1/N_c^3$. Thus, for example, taking $\psi_\ell \simeq 10^{-1}$, and taking into account that $2n_f T_R/3 = 1$ for $n_f = 3$, the coefficient a_2 defined in (24d) and which also appears in the right-hand side of (61) would be modified to the close value $a_2 \approx 0.07$. Finally, since in the above

$$\begin{aligned} & \ldots + \frac{2n_f T_R}{3N_c}\frac{C_F}{N_c}\left(\frac{C_F}{N_c} - 1\right)(a_1 - \tilde{a}_1)\gamma_0^2(G_1G_2)_\ell \\ & \approx -0.01 \times \gamma_0^2(G_1G_2)_\ell, \end{aligned}$$

b_2 defined in (62) would be changed to the value $b_2 \approx 0.17$, which only represents a 1% variation.

The derivatives of (H1) and (H2) with respect to ℓ are therefore, respectively, approximated by

$$\begin{aligned} Q_\ell &= \frac{C_F}{N_c}G_\ell + \mathcal{O}(\gamma_0^2), \\ Q_\ell^{(2)} &= \frac{C_F}{N_c}G_\ell^{(2)} + \frac{C_F}{N_c}\left(\frac{C_F}{N_c} - 1\right)(G_1G_2)_\ell + \mathcal{O}(\gamma_0^2), \end{aligned} \tag{H4}$$

because the inclusion of higher-order contributions (coming from the derivatives of the above $\mathcal{O}(\gamma_0)$ terms) in the nonsingular parts of the equations (such as (17), (20), (52), and (57)) would yield corrections beyond the precision of our approach.

APPENDIX I: LOGARITHMIC DERIVATIVES OF THE INCLUSIVE SPECTRUM

The logarithmic derivatives of G, that are used in Sec. V C, read

$$\begin{aligned} G_\ell^{(2)} &= \mathcal{C}_g G_1G_2(\chi_\ell + \psi_{1,\ell} + \psi_{2,\ell}), \\ (G_1G_2)_\ell &= G_1G_2(\psi_{1,\ell} + \psi_{2,\ell}), \\ G_{\ell\ell}^{(2)} &= \mathcal{C}_g G_1G_2[(\chi_\ell + \psi_{1,\ell} + \psi_{2,\ell})^2 \\ &\quad + \chi_{\ell\ell} + \psi_{1,\ell\ell} + \psi_{2,\ell\ell}], \\ (G_1G_2)_{\ell\ell} &= G_1G_2[(\psi_{1,\ell} + \psi_{2,\ell})^2 + \psi_{1,\ell\ell} + \psi_{2,\ell\ell}]. \end{aligned}$$

The functions introduced in (64) and (73) are the following:

$$\begin{aligned} f_1(\ell_1, \ell_2; \eta) &= (\psi_{1,\ell} + \psi_{2,\ell} + \chi_\ell)^2 + \psi_{1,\ell\ell} + \psi_{2,\ell\ell} - \beta_0\gamma_0^2(\psi_{1,\ell} + \psi_{2,\ell} + \chi_\ell) + \chi_{\ell\ell} = \mathcal{O}(\gamma_0^2), \\ f_2(\ell_1, \ell_2; \eta) &= (\psi_{1,\ell} + \psi_{2,\ell})^2 + \psi_{1,\ell\ell} + \psi_{2,\ell\ell} - \beta_0\gamma_0^2(\psi_{1,\ell} + \psi_{2,\ell}) = \mathcal{O}(\gamma_0^2), \\ f_3(\ell_1, \ell_2; \eta) &= 2\psi_{1,\ell}\psi_{2,\ell} + 2\chi_\ell(\psi_{1,\ell} + \psi_{2,\ell}) + \chi_{\ell\ell} + \chi_\ell^2 - \beta_0\gamma_0^2\chi_\ell = \mathcal{O}(\gamma_0^2), \\ f_4(\ell_1, \ell_2; \eta) &= \psi_{i,\ell}^2 + \psi_{i,\ell\ell} - \beta_0\gamma_0^2\psi_{i,\ell} = \mathcal{O}(\gamma_0^2). \end{aligned} \tag{I1}$$

[1] Yu. L. Dokshitzer, V. S. Fadin, and V. A. Khoze, Phys. Lett. B **115**, 242 (1982); Ya. I. Azimov, Yu. L. Dokshitzer, V. A. Khoze, and S. I. Troian, Z. Phys. C **31**, 213 (1986); C. P. Fong and B. R. Webber, Phys. Lett. B **229**, 289 (1989).

[2] V. A. Khoze and W. Ochs, Int. J. Mod. Phys. A **12**, 2949

(1997).
[3] Ya. I. Azimov, Yu. L. Dokshitzer, V. A. Khoze, and S. I. Troian, Z. Phys. C **27**, 65 (1985); Yu. L. Dokshitzer, V. A. Khoze, and S. I. Troian, J. Phys. G **17**, 1585 (1991).
[4] R. Pérez Ramos and B. Machet, J. High Energy Phys. 04 (2006) 043.
[5] R. Pérez Ramos, J. High Energy Phys. 06 (2006) 019 and references therein.
[6] R. Pérez Ramos, J. High Energy Phys. 09 (2006) 014.
[7] S. Jindariani, A. Korytov, and A. Pronko (CDF Collaboration), CDF Report No. CDF/ANAL/JET/PUBLIC/8406, 2007; http://www-cdf.fnal.gov/physics/new/qcd/ktdistributions_06/cdf8406_Kt_jets _public.pswww-cdf.fnal.gov/physics/new/qcd/ktdistributions_06/cdf8406_Kt _jets_public.ps.
[8] Yu. L. Dokshitzer, V. A. Khoze, A. H. Mueller, and S. I. Troyan, *Basics of Perturbative QCD* (Editions Frontières, Gif-sur-Yvette, 1991).
[9] F. Cuypers and K. Tesima, Z. Phys. C **54**, 87 (1992).
[10] Yu. L. Dokshitzer, Phys. Lett. B **305**, 295 (1993).
[11] F. Arleo, R. Pérez-Ramos, and B. Machet, Phys. Rev. Lett. **100**, 052002 (2008).
[12] V. A. Khoze, S. Lupia, and W. Ochs, Phys. Lett. B **386**, 451 (1996).
[13] J. Abdallah *et al.* (DELPHI Collaboration), Phys. Lett. B **605**, 37 (2005).
[14] I. M. Dremin, Phys. Usp. **37**, 715 (1994); I. M. Dremin and J. W. Gary, Phys. Rep. **349**, 301 (2001).
[15] S. Lupia and W. Ochs, Phys. Lett. B **418**, 214 (1998).
[16] M. Z. Akrawy *et al.* (OPAL Collaboration), Phys. Lett. B **247**, 617 (1990).
[17] NMLLA corrections arising from varying $\Lambda_{\rm QCD}$ are studied in detail in subsection III E.
[18] Furthermore, if one formally expands $\alpha_s = 2\pi/[4N_c\beta_0(\ln z + \ldots)]$ in powers of $\ln z$, the resulting first nonleading term $\propto 1/(\ln z + \ldots)^2$ yields an extra α_s^2 which only starts contributing at next-to-next-to-MLLA, out of the scope of the present work.
[19] F. E. Low, Phys. Rev. **110**, 974 (1958); T. H. Burnett and N. M. Kroll, Phys. Rev. Lett. **20**, 86 (1968).
[20] I. M. Dremin and V. A. Nechitailo, Mod. Phys. Lett. A **9**, 1471 (1994).
[21] In practice, these coefficients can be safely estimated by using the leading order formula $Q/G = C_f/N_c$ instead of (26) below. We checked that this approximation only marginally affects their values.
[22] Yu. L. Dokshitzer, V. S. Fadin, and V. A. Khoze, Z. Phys. C **18**, 37 (1983).
[23] Finding the analytical solution of these equations including NMLLA corrections is beyond the scope of this paper.
[24] Yu. L. Dokshitzer, V. A. Khoze, and S. I. Troian, Z. Phys. C **55**, 107 (1992); Yu. L. Dokshitzer, V. A. Khoze, and S. I. Troian, Int. J. Mod. Phys. A **7**, 1875 (1992); V. A. Khoze, W. Ochs, and J. Wosieck, arXiv:hep-ph/0009298, and references therein.
[25] The basic process under consideration is accordingly the emission of two hadrons, h_1 and h_2, inside a jet produced in a high-energy collision. Since the notations and kinematics are identical to the ones used in [4], the reader is referred to this work for a more detailed description.
[26] Taking into account the running of α_s, which increases with the evolution of the jet, goes *a priori* in the opposite way of increasing the hadronic yield with respect to the case where one freezes the coupling constant at the collision energy.
[27] Its role was found very small in the calculation of the $k_\perp$-distribution, such that, in practice, it was taken to be vanishing.
[28] See Ref. [7] and S. Jindariani (private communication).
[29] We recall that we only used the NMLLA solution of the evolution equations for the inclusive spectrum. All calculated NMLLA corrections to the $k_\perp$ distribution occur by the sole expansion of $\frac{x}{u}D_{\rm A}^h(\frac{x}{u},\ldots)$ at small x/u around $\ln u \approx \ln 1$ in the convolution (29).
[30] B. Alessandro *et al.* (ALICE Collaboration), J. Phys. G **32**, 1295 (2006).
[31] D. d'Enterria *et al.* (CMS Collaboration), J. Phys. G **34**, 2307 (2007).
[32] K. Konishi, A. Ukawa, and G. Veneziano, Nucl. Phys. **B157**, 45 (1979).
[33] I. M. Dremin, Phys. Lett. B **313**, 209 (1993).
[34] C. P. Fong and B. R. Webber, Nucl. Phys. **B355**, 54 (1991); Phys. Lett. B **241**, 255 (1990).
[35] I. M. Dremin, Acta Phys. Pol. B **35**, 417 (2004).
[36] Z. Koba, H. B. Nielsen, P. Olesen, Nucl. Phys. **B40**, 317 (1972)
[37] P. D. Acton *et al.* (OPAL Collaboration), Phys. Lett. B **287**, 401 (1992).
[38] T. Aaltonen *et al.* (CDF Collaboration), arXiv:0802.3182.
[39] S. Albino, B. A. Kniehl, G. Kramer, and W. Ochs, Phys. Rev. D **73**, 054020 (2006).
[40] Yu. L. Dokshitzer, G. Marchesini, and G. P. Salam, Phys. Lett. B **634**, 504 (2006).
[41] R. K. Ellis, W. J. Stirling, and B. R. Webber, *QCD and Collider Physics*, Cambridge Monographs in Particle Physics, Nuclear Physics and Cosmology Vol. 8 (Cambridge University Press, Cambridge, England, 1996); see, in particular, Eqs. (4.122) and (6.22).